Iterative methods for scattering problems in unbounded elastic waveguides

Vahan Baronian, Anne-Sophie Bonnet-Ben Dhia, Sonia Fliss, Antoine Tonnoir

Iterative methods for scattering problems in unbounded elastic waveguides

Vahan Baronian[a], Anne-Sophie Bonnet-Ben Dhia[b], Sonia Fliss[b,1], Antoine Tonnoir[a,b]

[a] *CEA, LIST, Gif-sur-Yvette, France*
[b] *POEMS (UMR CNRS-ENSTA Paristech-INRIA), 828 Boulevard des Maréchaux, Palaiseau, France*
[c] *E-mail: sonia.fliss@ensta-paristech.fr*

Abstract

We consider the time-harmonic problem of the diffraction of an incident propagative mode by a localized defect, in an infinite straight isotropic elastic waveguide. We propose several iterative algorithms to compute an approximate solution of the problem, using a classical finite element discretization in a small area around the perturbation, and a modal expansion in unbounded straight parts of the guide. Each algorithm can be related to a so-called domain decomposition method, with or without an overlap between the domains. Specific transmission conditions are used, so that only the sparse finite element matrix has to be inverted, the modal expansion being obtained by a simple projection, using the Fraser bi-orthogonality relation. The benefit of using an overlap between the finite element domain and the modal domain is emphasized, in particular for the extension to the anisotropic case. Numerical validations for two- and three-dimensional configurations for both isotropic and anisotropic media, are finally presented.

Keywords: elastic waveguide, diffraction, modal expansion, domain decomposition method, iterative methods

1. Introduction

The development of non destructive testing techniques using ultrasonic guided waves (see [23] and the references herein) motivates the improvement of existing numerical methods of simulation. In particular, efficient methods are required to compute the scattering of guided waves by arbitrary defects in elastic waveguides. Classically, the waveguide is supposed to be infinite and perfectly uniform, except in a bounded area containing the defect. A natural objective is to reduce the finite element computations to a region as closed as possible to this perturbed area. The difficulty is then to handle the artificial boundaries of the finite element domain in order to avoid spurious reflections. This is an old problematic [13] which has been satisfactorily solved in case of scalar equations, but still raises open questions for vectorial equations arising in electromagnetic or elastic waveguides. For scalar problems, two classes of methods can be used. Let us explain for each of them what are the specific issues when considering elastic waveguides.

A first class of methods consists in putting on each side of the perturbed area a perfectly matched ab-

sorbing layer (PML), so that the computed diffracted field almost vanishes at the end of the layer. This technique is easy to integrate in commercial codes (no specific implementation is needed) and leads to solve a classical sparse linear system. Unfortunately, it is well-known that PMLs do not work in elastic waveguides [34] because of the existence in some range of frequencies of inverse modes, whose group and phase velocities are of opposite signs. In such configuration, the PMLs do not select the correct outgoing solution. A remedy has been proposed and analyzed in [6] where the physical solution is reconstructed a posteriori by combining several wrong fields computed with PMLs. An alternative consists in using adiabatic viscoelastic absorbing layers [8] which are not perfectly matched but are sufficiently large to avoid spurious reflections. The main drawback of this approach is its cost since very large layers are required to get accurate results. Also let us point out that absorbing layer techniques (perfectly matched or not) require a fine adjustment of some parameters, which may limit their systematic use in an industrial context. Let us finally mention a more recent method for elastic waveguides based on Hardy space infinite elements [26].

A second possibility consists in using the modal decomposition of the field outside the perturbed area to derive transparent boundary conditions on the artificial boundaries of the finite element domain. The advantage is that such conditions are exact (and with an exponentially small error at the discrete level if enough modes are kept in the modal expansion). Different ways to implement such conditions have been proposed in the literature. In [36, 37], a formulation involving both finite elements and modal unknowns is derived, while only one type of unknowns in generally kept, modal unknowns in [24, 17] and finite elements unknowns in [4]. For the latter, the difficulty is due to a lack of orthogonality of the displacement fields associated to elastic modes. As a consequence, it is not possible to obtain a diagonal expression of the natural Dirichlet to Neumann operator (relating the normal stress to the displacement) in elastic waveguides. An alternative has been proposed in [4] (see [2] for more details and [5, 3] for applications), where the authors derived transparent boundary conditions relating hybrid displacement/stress vectors. This work is based on a bi-orthogonality relation, mixing displacement and stress components (which has been derived first by Fraser in 2D [11] and then extended to the 3D case [18]). Let us point out that a scalar Lagrange multiplier has to be introduced on the artificial boundaries, because these transparent conditions are not naturally compatible with the variational formulation in the perturbed area. The method is very accurate but requires a specific heavy implementation and leads to a partially dense linear system. Such system can be difficult to invert, in particular for elastic $3D$ configurations. Moreover, this approach cannot be used to the general anisotropic case.

In our work, we intend to gather advantages of both classes of methods. In other words, we would like to design a method using transparent boundary conditions based on modal expansions and such that only simple and sparse systems have to be inverted. A natural idea is to use iterative algorithms instead of direct

ones to solve a system involving transparent boundary conditions. This idea has been already applied to several problems set in unbounded domains [14, 15, 16]. A main feature is that the system to invert (or equivalently the preconditioner) is chosen as a sparse part of the complete system. As a consequence, the dense part of the matrix coming from the non-local transparent condition is involved only in the matrix-vector product step. It is also instructive to relate these iterative algorithms to domain decomposition methods. The specificity is that only two subdomains are introduced, a bounded one and an unbounded one where the equation can be explicitly solved, using an analytical representation (a modal expansion or an integral representation for instance). Different algorithms are derived by modifying the transmission conditions between the two-subdomains, which can overlap or not. This is now well known that this type of algorithms does not converge in general for time harmonic wave equation [16] but they can be used to design a preconditioned Krylov methods like GMRES [32]. The main criterion to discriminate between different algorithms is the rate of convergence of the associated GMRES algorithms.

In the present paper, we want to adapt these ideas to the case of elastic waveguides, which has not been considered in the literature. Combining such point of view with the ideas of [4], we derive new families of modal transparent boundary conditions. The benefit of adding an overlap is emphasized. Besides classical effects (for instance improvement of the convergence rate of associated iterative algorithms), it allows the construction of a particularly efficient transparent boundary condition in Section 7. Last but not least, this condition can be used for anisotropic waveguides. This is the main contribution of the paper.

The paper is organized as follows. In Section 2, the main notions concerning elastic modes are summarized and the solution of a given boundary value problem in a semi-infinite straight waveguide is derived. A first domain decomposition method, without overlapping, is introduced in Section 3. The three subdomains are two semi-infinite straight waveguides and a bounded domain containing the defect. The choice of the boundary conditions for each subproblem is motivated. This is generalized in Section 4 to a domain decomposition method with overlapping. The link between domain decomposition methods and transparent boundary conditions is done in Section 5. The convergence of the Schwarz algorithm is analyzed in Section 6, first in a simple model case where analytical formulas are available, and then in the general case. It appears that the convergence cannot be ensured, which leads to consider the previous domain decomposition as a preconditioner for a GMRES solution. At this stage, all the ingredients are gathered to present and analyze in Section 2 the so-called modal Outgoing transmission condition which compared to the other condition collects all the advantages. Two- and three-dimensional numerical results are finally presented in Section 8.

2. Modal analysis

2.1. Modes classification and Fraser bi-orthogonality relation

Let us consider a homogeneous isotropic elastic waveguide of section S in $\mathbf{x}_s$ plane - S is a bounded domain of $\mathbb{R}$ ($\mathbf{x}_s = x$) in the *2D case* or $\mathbb{R}^2$ ($\mathbf{x}_s = (x, y)$) in the *3D case*- and of axis z, which occupies the domain $S \times \mathbb{R}$ of $\mathbb{R}^2$ or $\mathbb{R}^3$. The density of the material denoted by ρ and the Lamé's coefficients denoted by λ and μ are supposed to be independent of z, but they may depend on $\mathbf{x}_s$. Finally, we suppose that the waveguide has a stress-free boundary $\partial S \times \mathbb{R}$. In time harmonic regime (of pulsation ω), the propagation in the waveguide is modelized by the following classical equations

$$\begin{cases} -\mathrm{div}\,\sigma(\mathbf{u}) - \omega^2 \rho\, \mathbf{u} = 0 & \text{in} \quad S \times \mathbb{R}, \\ \sigma(\mathbf{u}) \cdot \nu = 0 & \text{on} \quad \partial S \times \mathbb{R}, \end{cases} \tag{1}$$

where $\mathbf{u}$ represents the displacement field ($\mathbf{u} = (u_x, u_z)$ in the *2D case* and $\mathbf{u} = (u_x, u_y, u_z)$ in the *3D case*) and $\sigma(u)$ the stress tensor which is related to the strain tensor $\varepsilon(\mathbf{u}) = 1/2\,(\nabla \mathbf{u} + \nabla^T \mathbf{u})$ by Hooke's law

$$\sigma(\mathbf{u}) = \lambda\, \mathrm{div}\,(\mathbf{u})\, \mathrm{Id} \,+\, 2\,\mu\, \varepsilon(\mathbf{u}). \tag{2}$$

The vector ν denotes the outward unitary normal to $\partial\Omega$.

We remind in this section the convenient formalism introduced in [27, 28, 29] for the 2D case and extended in [2, 4] to the 3D case. First we denote by $\mathbf{u}_s$ the transverse part of the displacement field $\mathbf{u}$, $\mathbf{t}_s$ the transverse part of the axial stress $\sigma(\mathbf{u}) \cdot \mathbf{e}_z$, σ_s the transverse part of the stress tensor and ε_s the transverse part of the strain tensor :

$$\begin{aligned} &\text{in 2D :} \quad \mathbf{u}_s = u_x, \qquad \mathbf{t}_s = \sigma_{zx}, \qquad \sigma_s = \sigma_{xx}, \qquad \varepsilon_s = \varepsilon_{xx}, \\ &\text{in 3D :} \quad \mathbf{u}_s = \begin{bmatrix} u_x \\ u_y \end{bmatrix}, \quad \mathbf{t}_s = \begin{bmatrix} \sigma_{zx} \\ \sigma_{zy} \end{bmatrix}, \quad \sigma_s = \begin{bmatrix} \sigma_{xx} & \sigma_{xy} \\ \sigma_{yx} & \sigma_{yy} \end{bmatrix}, \quad \varepsilon_s = \begin{bmatrix} \varepsilon_{xx} & \varepsilon_{xy} \\ \varepsilon_{yx} & \varepsilon_{yy} \end{bmatrix}. \end{aligned}$$

Finally we set $t_z = -\sigma_{zz}$ and we define the two vectors

$$\mathbf{X} = \begin{bmatrix} \mathbf{t}_s \\ u_z \end{bmatrix} \quad \text{and} \quad \mathbf{Y} = \begin{bmatrix} \mathbf{u}_s \\ t_z \end{bmatrix},$$

which are hybrid in the sense that they mix displacement field and stress field components.

The modes of the waveguide are solutions of (1) with separated variables of the standard form

$$\mathbf{u}(\mathbf{x}_s, z) = \mathcal{U}(\mathbf{x}_s)\, e^{\imath \beta z},$$

where the function $\mathcal{U}$ and the complex number β are respectively the field profile and the propagation constant of the mode. It can be proved that there is a discrete family of rightgoing modes $(\beta_k, \mathcal{U}_k^+(\mathbf{x}_s))$, $k = 1, 2, \cdots$, and a corresponding family of leftgoing modes $(-\beta_k, \mathcal{U}_k^-(\mathbf{x}_s))$. Among these modes, one can distinguish a finite number of propagative modes such that $\beta_k \in \mathbb{R}$ and an infinite set of (possibly oscillating) evanescent modes such that $\beta_k \in \mathbb{C}\backslash\mathbb{R}$. For the propagative modes, the direction of propagation is given by the sign of the group velocity, and for the evanescent modes by the sign of the imaginary part of β_k. Then, by the adopted convention the propagative rightgoing modes verify $\dfrac{\partial \beta_k}{\partial \omega} > 0$ and the evanescent rightgoing modes $\mathrm{Im}(\beta_k) > 0$.

We conjecture in this paper that for the evanescent modes, we have

$$\lim_{k \to +\infty} \mathrm{Im}(\beta_k) = +\infty. \tag{3}$$

This conjecture is true for the particular case of Lamb's modes (see for instance [25]).

In terms of $\mathbf{X}$ and $\mathbf{Y}$ variables, for simple symmetry reasons, the rightgoing and leftgoing modes are of the form $(\beta_k, \mathcal{X}_k(\mathbf{x}_s), \mathcal{Y}_k(\mathbf{x}_s))$ and $(-\beta_k, -\mathcal{X}_k(\mathbf{x}_s), \mathcal{Y}_k(\mathbf{x}_s))$. As mentioned in the introduction, a difficulty comes from the fact that the modal transverse displacement fields $\mathcal{U}_k^{\pm}$ are not orthogonal in $L^2(S)$. But the modes satisfy however a bi-orthogonality relation, known as the Fraser's biorthogonality relation (see [11, 18]), that takes the simple following expression in terms of $\mathbf{X}$ and $\mathbf{Y}$ variables:

$$\int_S \mathcal{X}_\ell(\mathbf{x}_s)\, \mathcal{Y}_k(\mathbf{x}_s)\, d\mathbf{x}_s = 0 \quad \text{for} \quad \ell \neq k. \tag{4}$$

Except at the cutoff frequencies, the modes can be normalized so that we have finally:

$$\int_S \mathcal{X}_\ell(\mathbf{x}_s)\, \mathcal{Y}_k(\mathbf{x}_s)\, d\mathbf{x}_s = \delta_{k\ell}.$$

In the following, we suppose that ω is not a cut-off frequency.

2.2. The half-guide solution

Let us denote by Ω_a^+ the semi-infinite straight waveguide defined by $\Omega_a^+ = S \times \{z > a\}$. It will be useful in what follows to have a simple representation of the solution of equations (1) in Ω_a^+ for some given data on the boundary $\Gamma_a^+ = S \times \{z = a\}$.

More precisely, we will look for a solution which is a superposition of rightgoing modes, that we call an outgoing solution (since rightgoing modes propagate from Γ_a^+ to infinity). Such explicit solution is not available for classical boundary conditions, like Dirichlet condition on $\mathbf{u}$ for instance. Fraser relation (4) leads us to consider instead that $\mathbf{X}$ or $\mathbf{Y}$ is given on Γ_a^+.

Suppose for instance that $\mathbf{Y}$ is known on Γ_a^+ - in other words $\mathbf{u}_s$ and $t_z = -\sigma_{zz}$ - and let us denote by $\mathbf{Y}_a^+$ this data. Then, assuming some completeness of the modes (see [20]), we can expand $\mathbf{Y}_a^+$ on the $\mathcal{Y}_k$:

$$\mathbf{Y}_a^+ = \sum_{k>0} \alpha_k \, \mathcal{Y}_k,$$

and the value of α_k can be directly derived by using Fraser relation (4):

$$\alpha_k = \int_{\Gamma_a^+} \mathbf{Y}_a^+(\mathbf{x}_s) \, \mathcal{X}_k(\mathbf{x}_s) \, d\mathbf{x}_s.$$

Finally,

$$\mathbf{u}^+(\mathbf{x}_s, z) = \sum_{k>0} \left(\int_{\Gamma_a^+} \mathbf{Y}_a^+(\mathbf{x}_s) \, \mathcal{X}_k(\mathbf{x}_s) \, d\mathbf{x}_s \right) \mathcal{U}_k^+(\mathbf{x}_s) \, e^{\imath \beta_k (z-a)}, \tag{5}$$

is the outgoing solution of

$$\begin{cases} -\operatorname{div} \sigma(\mathbf{u}) - \omega^2 \rho \, \mathbf{u} = 0 & \text{in} \quad \Omega_a^+, \\ \sigma(\mathbf{u}) \cdot \nu = 0 & \text{on} \quad \partial\Omega_a^+, \\ \mathbf{Y} = \mathbf{Y}_a^+ & \text{on} \quad \Gamma_a^+. \end{cases} \tag{6}$$

Proceeding in the same way and setting

$$\Omega_a^- = S \times \{z < -a\} \quad \text{and} \quad \Gamma_a^- = S \times \{z = -a\},$$

we prove that

$$\mathbf{u}^-(\mathbf{x}_s, z) = \sum_{k>0} \left(\int_{\Gamma_a^-} \mathbf{Y}_a^-(\mathbf{x}_s) \, \mathcal{X}_k(\mathbf{x}_s) \, d\mathbf{x}_s \right) \mathcal{U}_k^-(\mathbf{x}_s) \, e^{-\imath \beta_k (z+a)}, \tag{7}$$

is the outgoing solution of

$$\begin{cases} -\operatorname{div} \sigma(\mathbf{u}) - \omega^2 \rho \, \mathbf{u} = 0 & \text{in} \quad \Omega_a^-, \\ \sigma(\mathbf{u}) \cdot \nu = 0 & \text{on} \quad \partial\Omega_a^-, \\ \mathbf{Y} = \mathbf{Y}_a^- & \text{on} \quad \Gamma_a^-. \end{cases} \tag{8}$$

Remark 2.1. *A similar expansion holds if we impose a condition of the type $\mathbf{X} = \mathbf{X}_a^\pm$ on $\Gamma_a^\pm$, where $\mathbf{X}_a^\pm$ is decomposed on the family $\mathcal{Y}_k(\mathbf{x}_s)$. However, to simplify the presentation, we will consider up to Section 7 the case of $\mathbf{Y}$ data on $\Gamma_a^\pm$ for solving the half-guide problem.*

2.3. The scattering problem

The notion of outgoing waves being introduced, we can define the scattering problem we will study in the sequel. Let us denote by Ω a locally perturbed waveguide defined by (see Figure 1) :

$$\Omega = \Omega_a^- \cup \Omega_a \cup \Omega_a^+ \quad \text{where} \quad \Omega_a = \Omega \cap \{|z| \leq a\}.$$

We suppose that Ω_a is a bounded domain and Ω is a connected domain. The scattering problem consists in finding the outgoing solution $\mathbf{u}$ of the following equations

$$\begin{cases} -\mathrm{div}\,\sigma(\mathbf{u}) - \omega^2 \rho\, \mathbf{u} = f & \text{in} \quad \Omega, \\ \sigma(\mathbf{u}) \cdot \nu = 0 & \text{on} \quad \partial S \times \mathbb{R}, \end{cases} \tag{9}$$

where f is a compactly supported source term whose support is included in Ω_a. In accordance with Section 2.2, we say that $\mathbf{u}$ is outgoing if it expands on the rightgoing modes in Ω_a^+, and on the leftgoing modes in Ω_a^- :

$$\mathbf{u} = \begin{cases} \sum_{k>0} \alpha_k^+ \mathcal{U}_k^+(\mathbf{x}_s)\; e^{\imath \beta_k (z-a)} & \text{in} \quad \Omega_a^+, \\ \sum_{k>0} \alpha_k^- \mathcal{U}_k^-(\mathbf{x}_s)\, e^{-\imath \beta_k (z+a)} & \text{in} \quad \Omega_a^-, \end{cases} \tag{10}$$

where $(\alpha_k^+)_k$ and $(\alpha_k^-)_k$ are two sequences of complex numbers. We define the scattering problem by equations (9-10). We suppose that ω is such that the scattering problem is well-posed.

Moreover, in the rest of the paper, the outgoing behavior of the solution in Ω_a^- and Ω_a^+ will be implicitly imposed for each problem set in these unbounded domains. So, we will refer to the scattering problem (9-10) only by (9).

3. A first domain decomposition approach

3.1. A multi-domain formulation

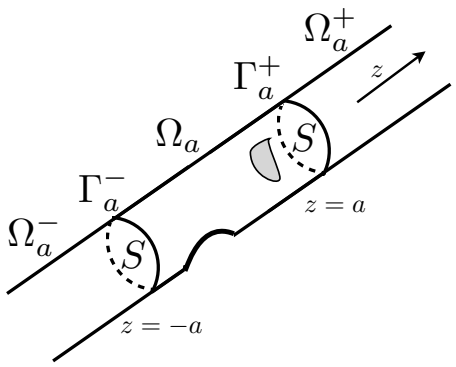

Figure 1: Geometry of Ω and notations

As shown on Figure 1, the domain Ω is decomposed into three parts and thanks to these three domains, we intend to write a multi-domain formulation of the scattering problem (9) which will be suitable for calculations. In the unbounded domains Ω_a^+ and Ω_a^-, the solution is represented thanks to the modal expansions

(5) and (7), and in Ω_a, since it is a bounded domain, we can use (for instance) a finite elements approximation of $\mathbf{u}$. Thus, we reformulate the scattering problem (9) with three problems set on the three domains $(\Omega_a^-, \Omega_a, \Omega_a^+)$ which will be coupled by their boundary conditions.

We can straightforwardly prove that $\mathbf{u}$ verifies the problem (9) if and only if $(u^- = u|_{\Omega_a^-}, u^a = u|_{\Omega_a}, u^+ = u|_{\Omega_a^+})$ are solutions of the equations

$$\begin{cases} -\operatorname{div}\sigma(\mathbf{u}^\pm) - \omega^2\rho\,\mathbf{u}^\pm = 0 & \text{in} \quad \Omega_a^\pm, \\ \sigma(\mathbf{u}^\pm)\cdot\nu = 0 & \text{on} \quad \partial\Omega\cap\partial\Omega_a^\pm, \end{cases} \begin{cases} -\operatorname{div}\sigma(\mathbf{u}^a) - \omega^2\rho\,\mathbf{u}^a = f & \text{in} \quad \Omega_a, \\ \sigma(\mathbf{u}^a)\cdot\nu = 0 & \text{on} \quad \partial\Omega\cap\partial\Omega_a, \end{cases} \tag{11}$$

with the transmission conditions

$$\begin{cases} \mathbf{u}^a = \mathbf{u}^\pm & \text{on} \quad \Gamma_a^\pm, \\ \sigma(\mathbf{u}^a)\cdot\nu = \sigma(\mathbf{u}^\pm)\cdot\nu & \text{on} \quad \Gamma_a^\pm, \end{cases} \tag{12}$$

that ensure the continuity of $\mathbf{u}$ and $\sigma(\mathbf{u}).\nu$ across the artificial boundaries $\Gamma_a^\pm$.

The modal expansion of $\mathbf{u}$ in the half-guide is expressed in terms of hybrid variables $\mathbf{X}$ and $\mathbf{Y}$ (see Section 2.2), so it will be useful to notice that the transmission conditions (12) can equivalently be rewritten as

$$\begin{cases} \mathbf{X}^a = \mathbf{X}^\pm & \text{on} \quad \Gamma_a^\pm, \\ \mathbf{Y}^a = \mathbf{Y}^\pm & \text{on} \quad \Gamma_a^\pm, \end{cases} \tag{13}$$

where $\mathbf{X}^a$ (resp. $\mathbf{Y}^a$) denotes $\mathbf{X}(\mathbf{u}^a)$ (resp. $\mathbf{Y}(\mathbf{u}^a)$) and $\mathbf{X}^\pm$ (resp. $\mathbf{Y}^\pm$) denotes $\mathbf{X}(\mathbf{u}^\pm)$ (resp. $\mathbf{Y}(\mathbf{u}^\pm)$).

3.2. The associated Schwarz algorithm

The first decomposition domain method was introduced by Schwarz [33] to solve a Laplace problem with non homogeneous Dirichlet boundary conditions, in a domain Ω which was the union of a disk and a rectangle. Since the Laplace equation is analytically solvable in a rectangle and in a disk, the key idea was to solve a Laplace problem iteratively in each domain and to prove that the process converges. Yet, to implement this process, boundary conditions must be chosen on the part of the boundary of the subdomains (the disk and the rectangle) not included in the boundary of the whole domain $\partial\Omega$. These choices define the iterative algorithm. In particular, the rate of convergence of the algorithm is strongly related to these choices.

This approach was extended to more general equations, in particular time harmonic scalar wave equations [10, 9, 12]. In that case and for a bounded domain, it has been proved that the Schwarz algorithm converges if Robin type conditions are imposed on the boundary of the subdomains. Yet, if one of the subdomain is unbounded, ensuring the convergence for the Helmholtz equation is not possible and only weak convergence can be proved using some relaxation techniques [7, 16].

In our case, the domain Ω is decomposed into three subdomains $(\Omega_a^-, \Omega_a, \Omega_a^+)$ and we consider the following class of iterative algorithms where $\mathbf{u}_{(n)}^a$ (resp. $\mathbf{u}_{(n)}^-$) denotes the solution in Ω_a (resp. $\Omega^\pm$) at the iteration n

$$\begin{cases} -\mathrm{div}\,\sigma(\mathbf{u}_{(n)}^a) - \omega^2\rho\,\mathbf{u}_{(n)}^a = f & \text{in } \Omega_a, \\ \sigma(\mathbf{u}_{(n)}^a)\cdot\nu = 0 & \text{on } \partial\Omega\cap\partial\Omega_a, \\ \mathcal{B}^a(\mathbf{u}_{(n)}^a) = \mathcal{B}^a(\mathbf{u}_{(n)}^\pm) & \text{on } \Gamma_a^\pm, \end{cases} \tag{14}$$

$$\begin{cases} -\mathrm{div}\,\sigma(\mathbf{u}_{(n)}^-) - \omega^2\rho\,\mathbf{u}_{(n)}^- = 0 & \text{in } \Omega_a^-, \\ \sigma(\mathbf{u}_{(n)}^-)\cdot\nu = 0 & \text{on } \partial\Omega\cap\partial\Omega_a^-, \\ \mathcal{B}^-(\mathbf{u}_{(n)}^-) = \mathcal{B}^-(\mathbf{u}_{(n-1)}^a) & \text{on } \Gamma_a^-, \end{cases} \qquad \begin{cases} -\mathrm{div}\,\sigma(\mathbf{u}_{(n)}^+) - \omega^2\rho\,\mathbf{u}_{(n)}^+ = 0 & \text{in } \Omega_a^+, \\ \sigma(\mathbf{u}_{(n)}^+)\cdot\nu = 0 & \text{on } \partial\Omega\cap\partial\Omega_a^+, \\ \mathcal{B}^+(\mathbf{u}_{(n)}^+) = \mathcal{B}^+(\mathbf{u}_{(n-1)}^a) & \text{on } \Gamma_a^+. \end{cases}$$

Here $\mathcal{B}^a$, $\mathcal{B}^+$ and $\mathcal{B}^-$ are the operators which define the boundary conditions and whose choice will be discussed below. We want to choose $\mathcal{B}^a$, $\mathcal{B}^+$ and $\mathcal{B}^-$ so that the algorithm (14) is **well-posed** and **consistent** in the following sense.

Definition 3.1. *The iterative process* (14) *with the associated boundary conditions defined by* $\mathcal{B}^a$, $\mathcal{B}^+$ *and* $\mathcal{B}^-$ *is*

- ***well-posed*** *if each of the three subproblems is well-posed,*
- ***consistent*** *if for any initial data, in case of convergence, the limits are solutions to* (11-12).

Obviously, the convergence of the algorithm is also required but this issue will be discussed in Section 6.

As we already explained in Section 2.2, to solve analytically the problems in the two half-guides Ω_a^- and Ω_a^+, we choose

$$\mathcal{B}^\pm(\mathbf{u}^\pm) = \mathbf{Y}^\pm \quad \text{on } \Gamma_a^\pm,$$

($\mathbf{X}$ is also possible, see Remark 2.1). With these choices, the problems set in $\Omega_a^\pm$ are well-posed, so to prove that the algorithm is **well-posed** it suffices to prove that the problem in Ω_a is well-posed as well.

In the domain Ω_a which contains the defect and the source term, we want to use a finite element method, so the boundary conditions on $\Gamma_a^\pm$ must be variational. Let us discuss two possibilities.

1. First, in order to have a **consistent** algorithm, it seems 'natural' to impose

$$\mathcal{B}^a(\mathbf{u}^a) = \mathbf{X}^a \quad \text{on } \Gamma_a^\pm, \tag{15}$$

so that, in case of convergence, the transmission conditions (13) and obviously the equations (11) are verified.

For the sake of clarity, let us emphasize that the boundary conditions $\mathcal{B}^a(\mathbf{u}^a_{(n)}) = \mathcal{B}^a(\mathbf{u}^\pm_{(n)})$ and $\mathcal{B}^\pm(\mathbf{u}^\pm_{(n)}) = \mathcal{B}^\pm(\mathbf{u}^a_{(n-1)})$ can be rewritten with classical notations as follows (see notation in Section 2.2):

$$\begin{pmatrix} (\mathbf{t}^a_{(n)})_s \\ (\mathbf{u}^a_{(n)})_z \end{pmatrix} = \begin{pmatrix} (\mathbf{t}^\pm_{(n)})_s \\ (\mathbf{u}^\pm_{(n)})_z \end{pmatrix} \quad \text{and} \quad \begin{pmatrix} (\mathbf{u}^\pm_{(n)})_s \\ (\mathbf{t}^\pm_{(n)})_z \end{pmatrix} = \begin{pmatrix} (\mathbf{u}^a_{(n-1)})_s \\ (\mathbf{t}^a_{(n-1)})_z \end{pmatrix}. \tag{16}$$

In particular, the condition (15) is a variational condition since it simply amounts to impose a part of the stress $\mathbf{t}_s$ and a part of the displacement field u_z (see Appendix Appendix B.1).

Besides, the well-posedness of the subproblem set in Ω_a can be proved except for a countable set of eigenfrequencies, thanks to the following lemma (see the proof in Appendix B.1).

Lemma 3.1. *The homogeneous problem*

$$\begin{cases} -\operatorname{div}\sigma(\mathbf{u}^a) - \omega^2\rho\,\mathbf{u}^a = 0 & \text{in} \quad \Omega_a, \\ \sigma(\mathbf{u}^a)\cdot\nu = 0 & \text{on} \quad \partial\Omega \cap \partial\Omega_a, \\ \mathbf{X}^a = 0 & \text{on} \quad \Gamma^\pm_a, \end{cases} \tag{17}$$

admits a countable set of eigenfrequencies.

2. A second choice, to have a **consistent** and **well-posed** algorithm for all frequencies, is to impose

$$\mathcal{B}^a(\mathbf{u}^a) = \sigma(\mathbf{u}^a)\cdot\nu + \alpha\,\mathbf{u}^a \quad \text{on} \quad \Gamma^\pm_a,$$

where α is a complex constant. In that case, the algorithm is **consistent** because if it converges, the transmission conditions (13) and the equations (11) are verified. Indeed, we can prove the following result.

Lemma 3.2. *The relations* (12) *(or* (13)*) are equivalent to*

$$\begin{cases} \mathbf{Y}^a = \mathbf{Y}^\pm & \text{on} \quad \Gamma^\pm_a, \\ \sigma(\mathbf{u}^a)\cdot\nu + \alpha\,\mathbf{u}^a = \sigma(\mathbf{u}^\pm)\cdot\nu + \alpha\,\mathbf{u}^\pm & \text{on} \quad \Gamma^\pm_a, \end{cases} \tag{18}$$

for any non-zero value of α.

Proof: The relations (18) can be rewritten as (see the notations in Section 2.2)

$$M_\alpha \begin{pmatrix} \mathbf{u}^a_s \\ t^a_z \\ \mathbf{t}^a_s \\ u^a_z \end{pmatrix} = M_\alpha \begin{pmatrix} \mathbf{u}^\pm_s \\ t^\pm_z \\ \mathbf{t}^\pm_s \\ u^\pm_z \end{pmatrix}, \quad \text{where} \quad M_\alpha = \begin{pmatrix} 1 & 0 & 0 & 0 \\ 0 & 1 & 0 & 0 \\ \alpha & 0 & 1 & 0 \\ 0 & 1 & 0 & \alpha \end{pmatrix}. \tag{19}$$

With the above expression, it is easy to understand that the equivalence between (18) and (13) is ensured if the matrix M is invertible, which holds for $\alpha \neq 0$. ■

Moreover, we can choose α such that the iterative process is **well-posed** for all frequencies by

Lemma 3.3. *For any value of α such that $Im\,\alpha \neq 0$, the problem*

$$\begin{cases} -\mathrm{div}\,\sigma(\mathbf{u}^a) - \omega^2 \rho\, \mathbf{u}^a = f & \text{in} \quad \Omega_a, \\ \sigma(\mathbf{u}^a)\cdot\nu = 0 & \text{on} \quad \partial\Omega \cap \partial\Omega_a, \\ \sigma(\mathbf{u}^a)\cdot\nu + \alpha\, \mathbf{u}^a = g & \text{on} \quad \Gamma_a^{\pm}, \end{cases} \tag{20}$$

is well-posed for any data f and g.

Proof: Let us first prove that the homogeneous problem admits as unique solution $\mathbf{u} = 0$. If the data f and g are null, then testing our equation with $\overline{\mathbf{u}}$ leads to (see Appendix B.1)

$$\mathrm{Im}\left(a(\mathbf{u}^a, \overline{\mathbf{u}}^a) + m(\mathbf{u}^a, \overline{\mathbf{u}}^a) + \alpha \int_{\Gamma_a^{\pm}} |\mathbf{u}^a|^2 \right) = \mathrm{Im}\,\alpha \int_{\Gamma_a^{\pm}} |\mathbf{u}^a|^2 = 0, \tag{21}$$

where the bilinear forms $a(\cdot,\cdot)$ and $m(\cdot,\cdot)$ have been defined in Appendix B.1.

Thus, we have $\mathbf{u}^a = 0$ and $\sigma(\mathbf{u}^a)\cdot\nu = 0$ (because $\sigma(\mathbf{u}^a)\cdot\nu + \alpha\,\mathbf{u}^a = 0$) on $\Gamma_a^{\pm}$, so by a unique continuation argument [38] we prove that $\mathbf{u}^a = 0$ in Ω_a. Finally, to prove that the problem (20) admits a solution for any data f and g, we notice that we can apply the Fredholm alternative and having proved that the problem has a unique solution, we therefore prove also the existence. ■

Let us sum up the two iterative algorithms we have described and their properties:

- First, we have considered

$$\begin{cases} \mathcal{B}^a(\mathbf{u}^a) = \mathbf{X}^a & \text{on} \quad \Gamma_a^{\pm}, \\ \mathcal{B}^{\pm}(\mathbf{u}^{\pm}) = \mathbf{Y}^{\pm} & \text{on} \quad \Gamma_a^{\pm}. \end{cases} \tag{22}$$

  Algorithm (14-22) is **consistent** and it is **well-posed** except for a discrete set of eigenfrequencies by Lemma 3.1,

- Second, we have considered

$$\begin{cases} \mathcal{B}^a(\mathbf{u}^a) = \sigma(\mathbf{u}^a)\cdot\nu + \alpha\,\mathbf{u}^a & \text{on} \quad \Gamma_a^{\pm}, \\ \mathcal{B}^{\pm}(\mathbf{u}^{\pm}) = \mathbf{Y}^{\pm} & \text{on} \quad \Gamma_a^{\pm}, \end{cases} \tag{23}$$

  For any value of α such that $\mathrm{Im}\,\alpha \neq 0$, Algorithm (14-23) is **consistent** by Lemma 3.2 and is also **well-posed** for all frequencies by Lemma 3.3.

4. The general domain decomposition approach

A natural generalization of the method proposed in the previous section is to consider that the three domains Ω_a^-, Ω_a and Ω_a^+ may overlap. Indeed, it is well known that for elliptic equations in bounded domains, the decomposition domain techniques have a geometrical rate of convergence which increases with the size of the overlapping, see [21].

4.1. Overlap and transmission conditions

Let us introduce

$$\Omega_b = \Omega \cap \{|z| < b\} \quad \text{where} \quad b - a = l > 0 \quad \text{and} \quad \Gamma_b^\pm = S \times \{z = \pm b\},$$

and denote by $B_l^\pm$ the overlapping areas between Ω_b and $\Omega_a^\pm$ (see Figure 2). As previously, we have to define

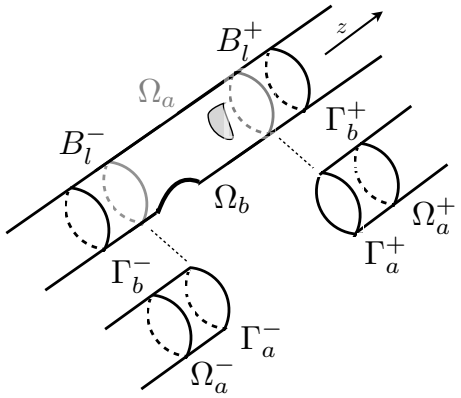

Figure 2: Decomposition of Ω and notations

four transmission conditions but now on the four cross-sections $(\Gamma_b^-, \Gamma_a^-, \Gamma_a^+, \Gamma_b^+)$. We consider a new class of iterative algorithms defined as follows

$$\begin{cases} -\mathrm{div}\,\sigma(\mathbf{u}_{(n)}^b) - \omega^2 \rho\, \mathbf{u}_{(n)}^b = f & \text{in } \Omega_b, \\ \sigma(\mathbf{u}_{(n)}^b) \cdot \nu = 0 & \text{on } \partial\Omega \cap \partial\Omega_b, \\ \mathcal{B}^b(\mathbf{u}_{(n)}^b) = \mathcal{B}^b(\mathbf{u}_{(n)}^\pm) & \text{on } \Gamma_b^\pm, \end{cases} \tag{24}$$

$$\begin{cases} -\mathrm{div}\,\sigma(\mathbf{u}_{(n)}^-) - \omega^2 \rho\, \mathbf{u}_{(n)}^- = 0 & \text{in } \Omega_a^-, \\ \sigma(\mathbf{u}_{(n)}^-) \cdot \nu = 0 & \text{on } \partial\Omega \cap \partial\Omega_a^-, \\ \mathcal{B}^-(\mathbf{u}_{(n)}^-) = \mathcal{B}^-(\mathbf{u}_{(n-1)}^b) & \text{on } \Gamma_a^-, \end{cases} \qquad \begin{cases} -\mathrm{div}\,\sigma(\mathbf{u}_{(n)}^+) - \omega^2 \rho\, \mathbf{u}_{(n)}^+ = 0 & \text{in } \Omega_a^+, \\ \sigma(\mathbf{u}_{(n)}^+) \cdot \nu = 0 & \text{on } \partial\Omega \cap \partial\Omega_a^+, \\ \mathcal{B}^+(\mathbf{u}_{(n)}^+) = \mathcal{B}^+(\mathbf{u}_{(n-1)}^b) & \text{on } \Gamma_a^+, \end{cases}$$

where $\mathcal{B}^b$, $\mathcal{B}^+$ and $\mathcal{B}^-$ are the operators that define the boundary conditions. We will consider two cases, similarly to the two algorithms previously described :

- for the first algorithm, we impose

$$\begin{cases} \mathcal{B}^b(\mathbf{u}^b) = \mathbf{X}^b & \text{on} \quad \Gamma_b^{\pm}, \\ \mathcal{B}^{\pm}(\mathbf{u}^{\pm}) = \mathbf{Y}^{\pm} & \text{on} \quad \Gamma_a^{\pm}. \end{cases} \tag{25}$$

- for the second algorithm, we impose

$$\begin{cases} \mathcal{B}^b(\mathbf{u}^b) = \sigma(\mathbf{u}^b)\cdot\nu + \alpha\,\mathbf{u}^b & \text{on} \quad \Gamma_b^{\pm}, \\ \mathcal{B}^{\pm}(\mathbf{u}^{\pm}) = \mathbf{Y}^{\pm} & \text{on} \quad \Gamma_a^{\pm}. \end{cases} \tag{26}$$

  for α such that $\operatorname{Im}\alpha \neq 0$.

For the **well-posedness**, the iterative algorithm (24-25) is similar to (14-22) and the algorithm (24-26) is similar to (14-23). Consequently, the process (24-25) is **well-posed** except for a countable set of eigenfrequencies (see Lemma 3.1) and the process (24-26) is **well-posed** for all frequencies (see Lemma 3.3). The **consistency** is not as obvious and is discussed in the next section 4.2.

Remark 4.1. *Let us notice that the overlap allows us to consider also the following boundary conditions :*

$$\begin{cases} \mathcal{B}^b(\mathbf{u}^b) = \mathbf{Y}^b & \text{on} \quad \Gamma_b^{\pm}, \\ \mathcal{B}^{\pm}(\mathbf{u}^{\pm}) = \mathbf{Y}^{\pm} & \text{on} \quad \Gamma_a^{\pm}. \end{cases} \tag{27}$$

Without overlapping, this case is impossible because it obviously does not lead to a ***consistent*** *algorithm. Even if this combination is possible in the overlapping case, we will not study here the corresponding algorithm since it has exactly the same properties as (24-25).*

4.2. The ***consistency*** *of the algorithms*

Without overlapping, to prove the **consistency** of the algorithm, it suffices to show that the limits satisfy the transmission relations (12). In the overlapping case, we must prove that the limits $\mathbf{u}^b$ and $\mathbf{u}^{\pm}$ (in case of convergence) coincide in the overlapping zones :

Definition 4.1. *The algorithms* (24-25) *and* (24-26) *are* ***consistent*** *if and only if every solutions of*

$$\begin{cases} -\operatorname{div}\sigma(\mathbf{u}^b) - \omega^2\rho\,\mathbf{u}^b = f & \text{in} \quad \Omega_b, \\ \sigma(\mathbf{u}^b)\cdot\nu = 0 & \text{on} \quad \partial\Omega\cap\partial\Omega_b, \\ \mathcal{B}^b(\mathbf{u}^b) = \mathcal{B}^b(\mathbf{u}^{\pm}) & \text{on} \quad \Gamma_b^{\pm}, \end{cases} \tag{28}$$

$$\begin{cases} -\operatorname{div}\sigma(\mathbf{u}^-) - \omega^2\rho\,\mathbf{u}^- = 0 & \text{in} \quad \Omega_a^-, \\ \sigma(\mathbf{u}^-)\cdot\nu = 0 & \text{on} \quad \partial\Omega\cap\partial\Omega_a^-, \\ \mathcal{B}^-(\mathbf{u}^-) = \mathcal{B}^-(\mathbf{u}^a) & \text{on} \quad \Gamma_a^-, \end{cases} \qquad \begin{cases} -\operatorname{div}\sigma(\mathbf{u}^+) - \omega^2\rho\,\mathbf{u}^+ = 0 & \text{in} \quad \Omega_a^+, \\ \sigma(\mathbf{u}^+)\cdot\nu = 0 & \text{on} \quad \partial\Omega\cap\partial\Omega_a^+, \\ \mathcal{B}^+(\mathbf{u}^+) = \mathcal{B}^+(\mathbf{u}^a) & \text{on} \quad \Gamma_a^+, \end{cases}$$

verify the compatibility relations

$$\mathbf{u}^b = \begin{cases} \mathbf{u}^- & \text{in} \quad B_l^-, \\ \mathbf{u}^+ & \text{in} \quad B_l^+. \end{cases} \tag{29}$$

Let us emphasize that if the two representations $\mathbf{u}^b$ and $\mathbf{u}^\pm$ of the solution in the overlapping areas $B_l^\pm$ verify the relations (29), then, denoting by $\mathbf{u}^a$ the restriction of $\mathbf{u}^b$ in Ω_a, the functions $(\mathbf{u}^-, \mathbf{u}^a, \mathbf{u}^+)$ are solutions to (11) and verify the transmission conditions (12). Thus, we recover the definition previously given of a **consistent** algorithm (see definition 3.1).

On the contrary, if the problem (28) admits a solution $(\mathbf{u}^-, \mathbf{u}^b, \mathbf{u}^+)$ that does not comply the compatibility relation (29), then by taking this solution as initial data of the iterative process (24-25) or (24-26), we get a stationary solution which does not comply (29) so the algorithm is not **consistent**.

Considering this definition, it seems natural to focus on the two differences $\mathbf{v}^\pm = \mathbf{u}^b - \mathbf{u}^\pm$ in $B_l^\pm$ which are solutions of the following problems set in B_l^- and B_l^+:

$$\begin{cases} -\mathrm{div}\,\sigma(\mathbf{v}^\pm) - \omega^2 \rho\, \mathbf{v}^\pm = 0 & \text{in} \quad B_l^\pm, \\ \sigma(\mathbf{v}^\pm)\cdot \nu = 0 & \text{on} \quad \partial\Omega \cap \partial B_l^\pm, \\ \mathcal{B}^b(\mathbf{v}^\pm) = 0 & \text{on} \quad \Gamma_b^\pm, \\ \mathcal{B}^\pm(\mathbf{v}^\pm) = 0 & \text{on} \quad \Gamma_a^\pm. \end{cases} \tag{30}$$

If the above problem is well-posed, i.e. $\mathbf{v}^\pm$ are necessarily 0, then the algorithm is **consistent** since the compatibility relations (29) are satisfied. In particular, choosing $\mathcal{B}^a$ and $\mathcal{B}^\pm$ as (25) and (26), and using the same arguments than in the proofs of Lemma 3.1 and Lemma 3.3, we have:

Lemma 4.2. 1. *The homogeneous problems* (30) *in* B_l^- *and* B_l^+ *with the boundary conditions* (25) *admit a countable set of eigenfrequencies. As a consequence, if* ω *is not an eigenfrequency of* (30-25)*, then the iterative process* (24-25) *is* ***consistent****.*

2. *The homogeneous problems* (30) *in* $B_l^\pm$ *with the conditions* (26) *have zero as unique solution. Therefore, we are ensured that for all frequencies, the algorithm* (24-26) *is* ***consistent****.*

We will prove now that the converse is true : if ω is an eigenfrequency of the homogeneous problem (30-25) then the algorithm (24-25) is not **consistent** in that case. First, let us give the following characterization of the eigenfrequencies:

Lemma 4.3. *The frequency* ω *is an eigenfrequency of* (30-25) *if and only if there is* k_0 *such that*

$$\beta_{k_0} l \equiv \frac{\pi}{2} \; mod\; (\pi), \tag{31}$$

where β_k is the axial wave number of the k-th mode at the frequency ω (see Section 2.2) and $l = b - a$. Moreover, the associated eigenfunctions in $B_l^{\pm}$ are proportional to

$$e^{\imath\beta_{k_0}(z\mp a)}\,\mathcal{U}_{k_0}^{+} - e^{-\imath\beta_{k_0}(z\mp a)}\,\mathcal{U}_{k_0}^{-}. \tag{32}$$

Proof: Since the calculations are the same in B_l^- and B_l^+, we will only make them in B_l^+. Let $\mathbf{v}^+$ be a solution of (30-25). Due to the regular geometry of B_l^+, $\mathbf{v}^+$ can be decomposed on the rightgoing and the leftgoing modes :

$$\begin{bmatrix} X(\mathbf{v}^+) \\ Y(\mathbf{v}^+) \end{bmatrix} = \sum_{k\geq 0} A_k^+\, e^{\imath\beta_k(z-a)} \begin{bmatrix} \mathcal{X}_k(\mathbf{x}_s) \\ \mathcal{Y}_k(\mathbf{x}_s) \end{bmatrix} + A_k^-\, e^{-\imath\beta_k(z-a)} \begin{bmatrix} -\mathcal{X}_k(\mathbf{x}_s) \\ \mathcal{Y}_k(\mathbf{x}_s) \end{bmatrix},$$

where $(A_k^-)_k$ and $(A_k^+)_k$ are two sequences of complex numbers. By Fraser's relation (4) and the boundary condition $Y(\mathbf{v}^+) = 0$ on Γ_a^+, we must verify for all k

$$A_k^- = -A_k^+,$$

and from the boundary condition $X(\mathbf{v}^+)$ on Γ_b^+, we get

$$A_k^+(e^{\imath\beta_k l} + e^{-\imath\beta_k l}) = 0.$$

which gives the result. ■

For these eigenfrequencies, the algorithm (24-25) is not **consistent**. Indeed, we prove in Appendix A the following proposition.

Proposition 4.4. *If ω is an eigenfrequency of* (30-25)*, then the limit problem* (28-25) *admits solutions that do not satisfy the compatibility relations* (29)*.*

Let us summarize the two new iterative algorithms we introduced and their properties :

- the first iterative problem (24-25) has a discrete set of frequencies for which it is not **well-posed** (see Lemma 3.1), and a second discrete set of frequencies for which it is not **consistent** (see Proposition 4.4).
- the second problem (24-26) is **well-posed** for all frequencies by Lemma 3.3 and also **consistent** for all frequencies by Lemma 4.2.

Remark 4.5. *The eigenfrequencies of the problem (24-26) and of the corresponding problem* (30) *are complex because α is complex. However some eigenfrequencies can come closer to the real axis. After discretization, the conditionning of the matrix would get worse near these frequencies. We notice again the influence of the resonances of the boxes. An appropriate choice of the parameter α can address this difficulty (see Section 8).*

5. From multi-domains formulation to transparent boundary conditions formulation

In the previous sections, we presented four algorithms that iteratively solve the problems set in each subdomain Ω_a^-, Ω_a or Ω_b and Ω_a^+. For all these algorithms, the resolutions in the half-guides $\Omega_a^\pm$ are direct since they only require to project the boundary data $\mathcal{B}^\pm(\mathbf{u}^\pm) = \mathbf{Y}^\pm$ on $\Gamma_a^\pm$ on the family of outgoing modes (see formula (5) and (7)). Thus, thanks to the modal expressions (5-7) of the solution in the half-guides, we can 'eliminate' the unknowns $\mathbf{u}^\pm$ and reformulate the iterative processes only in the bounded domain Ω_a or Ω_b.

In the following, in order to discuss generally the case without or with overlapping, we will suppose that b may be equal to a. So, when $b = a$ we will consider that $\mathcal{B}^b = \mathcal{B}^a$, $\Omega_b = \Omega_a$ and $\Gamma_b^\pm = \Gamma_a^\pm$.

Definition 5.1. *Let us denote by $\mathcal{T}_{Y\to X}^{\pm,l}$, the operator that maps a given data $\mathbf{Y}^\pm$ on $\Gamma_a^\pm$ to $\mathbf{X}^\pm = \mathbf{X}(\mathbf{u}^\pm)$ on $\Gamma_b^\pm$ where $\mathbf{u}^\pm$ is the rightgoing solution of* (6) *and* (8) *respectively in Ω_a^+ and Ω_a^-. It is defined by*

$$\mathcal{T}_{Y\to X}^{\pm,l}(\mathbf{Y}^\pm) = \pm \sum_{k>0} \left(\int_{\Gamma_a^\pm} \mathbf{Y}^\pm(\mathbf{x}_s)\, \mathcal{X}_k(\mathbf{x}_s)\, d\mathbf{x}_s \right) e^{\pm \imath \beta_k l}\, \mathcal{X}_k(\mathbf{x}_s), \tag{33}$$

where $l = b - a \geq 0$. Similarly, $\mathcal{T}_{Y\to R}^{+,l}$, is the operator that maps $\mathbf{Y}^\pm$ on $\Gamma_a^\pm$ to $\sigma(\mathbf{u}^\pm)\cdot\nu + \alpha\,\mathbf{u}^\pm$ on $\Gamma_b^\pm$.

Thanks to these operators, the iterative process (24), with the associated boundary conditions (25) and (26), can be equivalently rewritten only in the bounded domain Ω_b. For example, the problem (24-25) for $l \geq 0$ is equivalent to

$$\begin{cases} -\mathrm{div}\,\sigma(\mathbf{u}_{(n)}^b) - \omega^2 \rho\, \mathbf{u}_{(n)}^b = f & \text{in} \quad \Omega_b, \\ \sigma(\mathbf{u}_{(n)}^b)\cdot\nu = 0 & \text{on} \quad \partial\Omega \cap \partial\Omega_b, \\ \mathbf{X}_{(n)}^b \mp \mathcal{T}_{Y\to X}^{\pm,l}(\mathbf{Y}_{(n-1)}^b\big|_{\Gamma_a^\pm}) = 0 & \text{on} \quad \Gamma_b^\pm. \end{cases} \tag{34}$$

Let us note that this corresponds to an iterative algorithm to solve the direct problem

$$\begin{cases} -\mathrm{div}\,\sigma(\mathbf{u}^b) - \omega^2 \rho \mathbf{u}^b = f & \text{in} \quad \Omega_b, \\ \sigma(\mathbf{u}^b)\cdot\nu = 0 & \text{on} \quad \partial\Omega \cap \partial\Omega_b, \\ \mathbf{X}^b \mp \mathcal{T}_{Y\to X}^{\pm,l}(\mathbf{Y}^b\big|_{\Gamma_a^\pm}) = 0 & \text{on} \quad \Gamma_b^\pm. \end{cases} \tag{35}$$

For $l = 0$, the last problem was studied in [4]. In the present paper, we propose in some sense extensions of the condition considered in [4] (YtX without overlapping). In the next section, we study the advantages of the overlap with the intention of solving the problem using an iterative algorithm.

6. The convergence analysis

In this section, we will study the convergence of the iterative algorithms presented before. Even if we will see that the convergence cannot be ensured, the analysis helps to explain the benefit of the overlapping. To

begin, we will consider a particular geometry for which analytical calculations can be done. Then, we will generalize our results to the case of an arbitrary geometry by using more general but abstract arguments.

6.1. Analytical study in a simple case

We consider in this section an unperturbed half-guide (see Figure 3) $\Omega = S\times]0,\infty[$ and the problem

$$\begin{cases} -\operatorname{div}\sigma(\mathbf{u}) - \omega^2\rho\,\mathbf{u} = f & \text{in} \quad \Omega, \\ \sigma(\mathbf{u})\cdot\nu = 0 & \text{on} \quad \partial S\times]0,+\infty[, \\ \mathbf{X}(\mathbf{u}) = 0 & \text{on} \quad \Gamma_0 = S\times\{z=0\}. \end{cases} \tag{36}$$

The domain can be decomposed into two subdomains Ω_a^+ and $\Omega_b = S\times]0,b[$ with $l = b-a \geq 0$ and we consider the following class of iterative processes

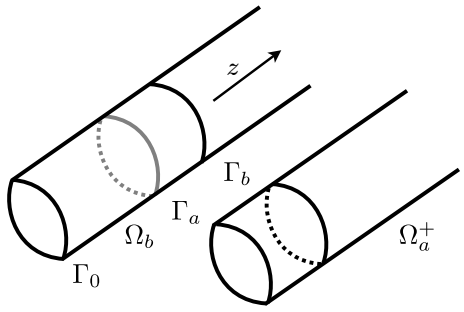

Figure 3: Geometry of the regular half-guide Ω, $3D$ case.

$$\begin{cases} -\operatorname{div}\sigma(\mathbf{u}^b_{(n)}) - \omega^2\rho\,\mathbf{u}^b_{(n)} = f & \text{in} \quad \Omega_b, \\ \sigma(\mathbf{u}^b_{(n)})\cdot\nu = 0 & \text{on} \quad \partial S\times]0,b[, \\ \mathbf{X}(\mathbf{u}^b_{(n)}) = 0 & \text{on} \quad \Gamma_0, \\ \mathcal{B}^b(\mathbf{u}^b_{(n)}) = \mathcal{B}^+(\mathbf{u}^+_{(n)}) & \text{on} \quad \Gamma_b = \Gamma_b^+, \end{cases} \quad \begin{cases} -\operatorname{div}\sigma(\mathbf{u}^+_{(n)}) - \omega^2\rho\,\mathbf{u}^+_{(n)} = 0 & \text{in} \quad \Omega_a^+, \\ \sigma(\mathbf{u}^+_{(n)})\cdot\nu = 0 & \text{on} \quad \partial S\times]a,+\infty[, \\ \mathcal{B}^+(\mathbf{u}^+_{(n)}) = \mathcal{B}^+(\mathbf{u}^b_{(n-1)}) & \text{on} \quad \Gamma_a = \Gamma_a^+. \end{cases} \tag{37}$$

where the boundary conditions $\mathcal{B}^b$ and $\mathcal{B}^+$ that can be imposed will be discussed. To study the convergence, it suffices to consider the case of a null source term f and we expect, for a non zero initial data, that $\mathbf{u}^b_{(n)}$ and $\mathbf{u}^+_{(n)}$ tend to 0 when n goes to $+\infty$.

In order to use the modal decomposition in Ω_a^+ and in Ω_b thanks to Fraser's relation (4), we impose

$$\begin{cases} \mathcal{B}^b(\mathbf{u}^b) = \mathbf{X}^b & \text{on} \quad \Gamma_b, \\ \mathcal{B}^+(\mathbf{u}^+) = \mathbf{Y}^+ & \text{on} \quad \Gamma_a. \end{cases} \tag{38}$$

Thus, we are able to compute analytically the solution of the algorithm (37-38) step by step and study its convergence.

The process (37-38) can be defined either without overlapping (i.e $a = b$) or with overlapping (i.e $a < b$). Let us remind the properties of the process (37-38) in this two cases :

- if $a = b$, then the process is similar to (14-22) and is **consistent** and **well-posed**, except for a discrete set of frequencies (see Lemma 3.1),
- if $a < b$, then the process is similar to (24-25) and is **consistent**, except for a discrete set of frequencies linked to the overlapping area (see Proposition 4.4), and is **well-posed**, except for a second discrete set of frequencies (see Lemma 3.1) that we will recover in the sequel.

To prove that $\mathbf{u}^b_{(n)}$ and $\mathbf{u}^+_{(n)}$ tend to 0 when n goes to $+\infty$, we can focus only on the boundaries and expect that $\mathcal{B}^b(\mathbf{u}^+_{(n)})$ on Γ_b and $\mathcal{B}^+(\mathbf{u}^b_{(n)})$ on Γ_a tend to zero. Let us consider for instance that $\mathcal{B}^b(\mathbf{u}^+_{(n)})$ is known (i.e $\mathbf{X}^+_{(n)}$ is known) on Γ_b and let us compute the next iteration $\mathcal{B}^b(\mathbf{u}^+_{(n+1)})$. This computation is done in three steps :

1. Thanks to the regular geometry of Ω_b and the Fraser's relation (4), we can solve the problem in Ω_b and, by the same technique used in the proof of Lemma 4.3, we get that

$$\mathbf{u}^b_{(n)} = \sum_{k\geq 0} \left(\int_{\Gamma_b} \mathbf{X}^+_{(n)}\, \mathcal{Y}_k \right) \frac{1}{e^{i\beta_k b} - e^{-i\beta_k b}} \left(\mathcal{U}^+_k(\mathbf{x}_s)\, e^{i\beta_k z} + \mathcal{U}^-_k(\mathbf{x}_s)\, e^{-i\beta_k z} \right). \tag{39}$$

Let us remark that in the above expression, the term $e^{i\beta_k b} - e^{-i\beta_k b}$ may vanish for a particular $\beta_{k_0}(\omega)$. This corresponds to the frequencies for which the problem set in Ω_b is not well-posed (see Lemma 3.1), which are excluded here.

2. Then, using $\mathcal{B}^+(\mathbf{u}^+_{(n+1)}) = \mathcal{B}^+(\mathbf{u}^b_{(n)})$ and thanks to the modal expansion (39), we get that $\mathcal{B}^+(\mathbf{u}^+_{(n+1)})$ on Γ_a is given by

$$\mathbf{Y}^+_{(n+1)} = \mathbf{Y}^b_{(n)} = \sum_{k\geq 0} \left(\int_{\Gamma_b} \mathbf{X}^+_{(n)}\, \mathcal{Y}_k \right) \frac{e^{\imath\beta_k a} + e^{-\imath\beta_k a}}{e^{\imath\beta_k b} - e^{-\imath\beta_k b}}\, \mathcal{Y}_k(\mathbf{x}_s). \tag{40}$$

3. Finally, from $\mathcal{B}^+(\mathbf{u}^+_{(n+1)}) = \mathbf{Y}^+_{(n+1)}$ on Γ_a, we get the modal expansion in the half-guide Ω^+_a (by formula (5)) and we easily deduce $\mathcal{B}^b(\mathbf{u}^+_{(n+1)})$ on Γ^+_b:

$$\begin{aligned} \mathbf{X}^+_{(n+1)} &= \sum_{k\geq 0} \left(\int_{\Gamma_a} \mathbf{Y}^+_{(n+1)}\, \mathcal{X}_k \right) \mathcal{X}_k(\mathbf{x}_s) e^{i\beta_k l} \\ &= \sum_{k\geq 0} \lambda_k \left(\int_{\Gamma_b} \mathbf{X}^+_{(n)}\, \mathcal{Y}_k \right) \mathcal{X}_k(\mathbf{x}_s). \end{aligned} \tag{41}$$

where

$$\forall k \in \mathbb{N}, \quad \lambda_k = \frac{1 + e^{-2i\beta_k a}}{1 - e^{-2i\beta_k (a+l)}}. \tag{42}$$

where $l = b - a$ is the length of the overlapping area. As usual, the convergence relies on the localization of the λ_k's with respect to the unit disk. The specific difficulty here is that the families $(\mathcal{X}_k)_k$ and $(\mathcal{Y}_k)_k$ are not orthonormal.

The properties of the λ_k are completely different for the cases without overlapping ($a = b$) and with overlapping ($b > a$), due to behaviour for the evanescent modes (see the conjecture (3))

$$\lim_{k \to +\infty} \mathrm{Im}(\beta_k) = +\infty.$$

- **Algorithm without overlapping** If $l = 0$, we have $e^{-2i\beta_k a} \to +\infty$ and therefore $\lim\limits_{k \to +\infty} \lambda_k = -1$ Even if all the λ_k's are by chance inside the unit circle, the algorithm can never converge geometrically.

- **Algorithm with overlapping** If $l > 0$, we have

  $$|\lambda_k| \underset{+\infty}{\sim} e^{-2\mathrm{Im}(\beta_k) l}.$$

  Therefore, $|\lambda_k|$ tends to 0 exponentially fast and there are at most a finite number of λ_k with modulus greater than 1. By (41), we show easily that for all $\varepsilon \geq 0$

  $$\|\mathbf{X}^+_{(n+1)}\|_{L^2(S)} \leq \|\mathbf{X}^+_{(n)}\|_{L^2(S)} \sup_{k \in \mathbb{N}}(|\lambda_k| e^{\varepsilon \mathrm{Im}(\beta_k) l}) \sum_{k \in \mathbb{N}} e^{-\varepsilon \mathrm{Im}(\beta_k) l} \left[\|\mathcal{Y}_k\|^2 + \|\mathcal{X}_k\|^2\right].$$

  Note that for $\varepsilon = 0$, the serie in the right hand side diverges. We conjecture that the norm of $\mathcal{X}_k$ and $\mathcal{Y}_k$ grow at most polynomially so the serie converges for all $\varepsilon > 0$. If all the λ_k's are inside the unit disk, it exists $\varepsilon \in (0, 2)$ such that

  $$\sup_{k \in \mathbb{N}}(|\lambda_k| e^{\varepsilon \mathrm{Im}(\beta_k) l}) < 1$$

  and then the algorithm converges. But this condition can or cannot be satisfied depending on the configurations, so the convergence cannot be ensured systematically. However, we consider that the overlap has improved the situation as we will explain in the conclusion of this section.

To illustrate these results, we have represented on Figure 4 the localization of the coefficients λ_k in the complex plane, for a waveguide of width h made of aluminium (see [31] for the coefficients of the material), at a given frequency ω and for various sizes of the overlap l. The frequency is such that there are 6 propagative modes. The coefficients λ_k related to the propagative modes (resp. the evanescent modes) are represented by circles (resp. by stars). We can observe that, as we explained, for $l = 0$ the λ_k related to the evanescent modes accumulate at -1, and for $l > 0$, these coefficients λ_k accumulate at 0.

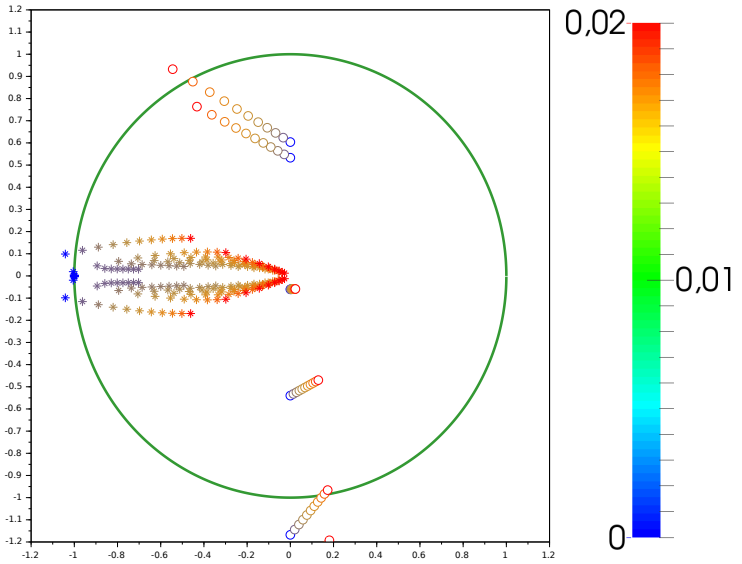

Figure 4: Localization of the coefficients λ_k in the complex plane : the color scale indicates l/h where h is the width of the waveguide and l the size of the overlap.

6.2. The general result

We consider again a semi infinite waveguide but contrary to the previous section, the geometry is arbitrary. Without loss of generality, we consider the following iterative process

$$\begin{cases} -\mathrm{div}\,\sigma(\mathbf{u}^b_{(n)}) - \omega^2\rho\,\mathbf{u}^b_{(n)} = f & \text{in} \quad \Omega_b, \\ \sigma(\mathbf{u}^b_{(n)})\cdot\nu = 0 & \text{on} \quad \partial\Omega_b \setminus \Gamma_b, \\ \sigma(\mathbf{u}^b_{(n)})\cdot\nu + \alpha\mathbf{u}^b_{(n)} = \sigma(\mathbf{u}^+_{(n)})\cdot\nu + \alpha\mathbf{u}^+_{(n)} & \text{on} \quad \Gamma_b, \end{cases} \quad \begin{cases} -\mathrm{div}\,\sigma(\mathbf{u}^+_{(n)}) - \omega^2\rho\,\mathbf{u}^+_{(n)} = 0 & \text{in} \quad \Omega^+_a, \\ \sigma(\mathbf{u}^+_{(n)})\cdot\nu = 0 & \text{on} \quad \partial\Omega^+_a \setminus \Gamma_a, \\ Y(\mathbf{u}^+_{(n)}) = Y(\mathbf{u}^b_{(n-1)}) & \text{on} \quad \Gamma_a. \end{cases}$$

Let us consider that $\sigma(\mathbf{u}^+_{(n)})\cdot\nu+\alpha\mathbf{u}^+_{(n)}$ is known on Γ_b and compute the next iteration $\sigma(\mathbf{u}^+_{(n+1)})\cdot\nu+\alpha\mathbf{u}^+_{(n+1)}$ on Γ_b.

1. One has to solve a problem of this form

$$\begin{cases} -\mathrm{div}\,\sigma(\mathbf{u}^b) - \omega^2\rho\mathbf{u}^b = 0 \quad \text{in} \quad \Omega_b, \\ \sigma(\mathbf{u}^b)\cdot\nu = 0 \quad \text{on} \quad \partial\partial\Omega_b \setminus \Gamma_b, \\ \sigma(\mathbf{u}^b)\cdot\nu + \alpha\mathbf{u}^b = g \quad \text{on} \quad \Gamma_b, \end{cases} \tag{43}$$

where g is a given data. This interior problem admits a unique solution that continuously depends on g, and we denote by $\mathcal{T}^b_{\mathcal{R}\to\mathcal{Y}}$ the operator that maps the Robin data g on Γ_b to the Y-data $Y(\mathbf{u}^b)$ on Γ_a where

$\mathbf{u}^b$ is solution of the above problem.

By definition, we have then

$$Y(\mathbf{u}^b_{(n)}) = \mathcal{T}^b_{\mathcal{R}\to\mathcal{Y}} \left[\sigma(\mathbf{u}^+_{(n)})\cdot\nu + \alpha\mathbf{u}^+_{(n)}\right]$$

2. By definition 5.1 of the operator $\mathcal{T}^{+,l}_{\mathcal{Y}\to\mathcal{R}}$, we extend the "iteration formula" (41)

$$\left[\sigma(\mathbf{u}^+_{(n+1)})\cdot\nu + \alpha\mathbf{u}^+_{(n+1)}\right] = \mathcal{T}^{+,l}_{\mathcal{Y}\to\mathcal{R}} \circ \mathcal{T}^b_{\mathcal{R}\to\mathcal{Y}} \left[\sigma(\mathbf{u}^+_{(n)})\cdot\nu + \alpha\mathbf{u}^+_{(n)}\right]$$

A necessary and sufficient condition for the convergence is that

$$\sup_{k\in\mathbb{N}} |\lambda_k| < 1$$

where the complex coefficients λ_k are the eigenvalues of the operators $\mathcal{T}^{+,l}_{\mathcal{Y}\to\mathcal{R}} \circ \mathcal{T}^b_{\mathcal{R}\to\mathcal{Y}}$.

Contrary to the regular case, we do not have any explicit information on λ_k. Yet, we can prove in the overlapping case that there are only a finite number of λ_k whose modulus is greater that 1. Indeed, if $l > 0$, as the operator $\mathcal{T}^{+,l}_{\mathcal{Y}\to\mathcal{R}} \circ \mathcal{T}^b_{\mathcal{R}\to\mathcal{Y}}$ is compact (see Lemma 6.1), its eigenvalue form a discrete set whose only point of accumulation is 0.

Due to the continuity of the operator $\mathcal{T}^b_{\mathcal{R}\to\mathcal{Y}}$, proving that $\mathcal{T}^{+,l}_{\mathcal{Y}\to\mathcal{R}} \circ \mathcal{T}^b_{\mathcal{R}\to\mathcal{Y}}$ is compact is achieved by the

Theorem 6.1. *Suppose for $l = b - a > 0$ that*

$$\sum_{k\in\mathbb{N}} e^{-\beta_k l} \left[\|\mathcal{Y}_k\|^2 + \|\mathcal{X}_k\|^2\right] < +\infty,$$

then the operator $\mathcal{T}^{+,l}_{\mathcal{Y}\to\mathcal{R}}$ is compact and consequently

$$\lim_{k\to+\infty} \lambda_k = 0.$$

Proof: The compactness of $\mathcal{T}^{+,l}_{\mathcal{Y}\to\mathcal{R}}$ is the consequence of the compactness of $\mathcal{T}^{+,l}_{\mathcal{Y}\to\mathcal{X}}$ and $\mathcal{T}^{+,l}_{\mathcal{Y}\to\mathcal{Y}}$. Let us show that for $\mathcal{T}^{+,l}_{\mathcal{Y}\to\mathcal{X}}$, the proof for $\mathcal{T}^{+,l}_{\mathcal{Y}\to\mathcal{Y}}$ being similar. It suffices to show that $\mathcal{T}^{+,l}_{\mathcal{Y}\to\mathcal{X}}$ is the limit of a sequence of following operators of finite rank

$$\mathcal{T}^{+,l,N}_{\mathcal{Y}\to\mathcal{X}}(\mathbf{Y}) = \sum_{k\geq 0}^{N} \left(\int_{\Gamma^{\pm}_a} \mathbf{Y}(\mathbf{x}_s)\mathcal{X}_k(\mathbf{x}_s)\, d\mathbf{x}_s\right) e^{i\beta_k l}\mathcal{X}_k(\mathbf{x}_s).$$

Using simple arguments (triangular and Cauchy-Schwartz inequalities), the hypothesis ensures the convergence. ■

Remark 6.2. *Obviously the result is wrong in absence of overlap ($l = 0$).*

6.3. Conclusion

The main result of this section is that thanks to the overlapping, the sequence of $(\lambda_k)_k$ concentrates around zero. We will see in Section 8 that this property will improve the rate of convergence of a GMRES algorithm where the preconditioner is constructed thanks to our iterative algorithms. Moreover it seems that larger is the overlap, larger will be the number of $(\lambda_k)_k$ around 0. We will see that consequently larger is the overlap, more rapid will be the convergence of the GMRES. However the preconditioner corresponds to a sparse matrix whose size depends on the size of the interior domain Ω^b. Then the overlap has a computational cost for the inversion of the preconditioner.

7. Achieving a complete efficiency with a modal 'outgoing' transmission condition

In the previous sections, we have explained how to design a good iterative algorithm, thanks to the overlaps $B_l^{\pm}$ and appropriate conditions on the exterior boundaries $\Gamma_b^{\pm}$. Thanks to the Fraser relation (4), the conditions $\mathcal{B}^{\pm}(\mathbf{u}^{\pm}) = \mathbf{Y}^{\pm}$ have the good property to provide the modal expansions of the solution in $\Omega_a^{\pm}$, as explained in Section 2.2. Moreover, the Robin condition $\mathcal{B}^b(\mathbf{u}^b) = \sigma(\mathbf{u}^b) + \alpha\mathbf{u}^b$ with a complex constant α makes the algorithm consistent since the associated problems in the boxes $B_l^{\pm}$ (cf problem (30)) are always well-posed (see Lemma 4.2). Finally, as seen in Section 6, the presence of the overlaps will a priori improve the convergence of a GMRES algorithm where the preconditioner is constructed thanks to our iterative algorithms (see Section 8 for more details).

We will now go further by changing the interior transmission conditions $\mathcal{B}^{\pm}(\mathbf{u}^{\pm})$. We will see below that considering instead non local transmission conditions also provides naturally the modal expansions and gathers all the following advantages :

1. it avoids spurious effects of the boxes $B_l^{\pm}$ (in particular the resonances mentioned in remark 4.5);
2. it improves the convergence of an associated GMRES algorithm independently of the size of the overlap;
3. last but not least, this approach has the advantage to be generalizable to **anisotropic** cases, contrary to the previous algorithms.

7.1. Description of the method

In the following, the explanations will be given for the transmission condition on Γ_a^+. Obviously, the same technique can be applied for the transmission condition on Γ_a^-.

Let us recall that the transmission conditions on Γ_a^+ and Γ_b^+ must ensure that we have the compatibility $\mathbf{u}^+ = \mathbf{u}^b$ in B_l^+ (see definition 4.1). The idea now is to use the modal expansions of both $\mathbf{u}^b$ and

$\mathbf{u}^+$ to express a non-local modal transmission condition. Due to the geometry of B_l^+, $\mathbf{u}^b$ and $\mathbf{u}^+$ can be decomposed *a priori* on the rightgoing and leftgoing modes

$$\begin{bmatrix} X(\mathbf{u}) \\ Y(\mathbf{u}) \end{bmatrix} = \sum_{k\geq 0} A_k^+(\mathbf{u})\, e^{\imath\beta_k(z-a)} \begin{bmatrix} \mathcal{X}_k(\mathbf{x}_s) \\ \mathcal{Y}_k(\mathbf{x}_s) \end{bmatrix} + A_k^-(\mathbf{u})\, e^{-\imath\beta_k(z-a)} \begin{bmatrix} -\mathcal{X}_k(\mathbf{x}_s) \\ \mathcal{Y}_k(\mathbf{x}_s) \end{bmatrix} \quad \text{in} \quad B_l^+, \tag{44}$$

where $\mathbf{u} = \mathbf{u}^b$ or $\mathbf{u}^+$, and $A_k^\pm(\mathbf{u})$ are the modal amplitudes of $\mathbf{u}$ given, thanks to the Fraser's relation (4), by

$$A_k^+(\mathbf{u}) = \frac{1}{2}\left(\int_{\Gamma_a^+} \mathbf{X}\,\mathcal{Y}_k + \int_{\Gamma_a^+} \mathbf{Y}\,\mathcal{X}_k\right) \quad \text{and} \quad A_k^-(\mathbf{u}) = \frac{1}{2}\left(\int_{\Gamma_a^+} \mathbf{Y}\,\mathcal{X}_k - \int_{\Gamma_a^+} \mathbf{X}\,\mathcal{Y}_k\right). \tag{45}$$

Since $\mathbf{u}^+$ should be outgoing in Ω_a^+, we propose to match :

$$A_k^+(\mathbf{u}^b) = A_k^+(\mathbf{u}^+). \tag{46}$$

Using formula (45), this condition is nothing else but a non-local condition involving the datas $\mathbf{X}$ and $\mathbf{Y}$ (or $(\mathbf{u}_s, u_z)$ and $(\mathbf{t}_s, t_z)$) taken on Γ_a^+. It means that rightgoing components of $\mathbf{u}^b$ and $\mathbf{u}^+$ coincide, so that $\mathbf{u}^b - \mathbf{u}^+$ is outgoing in the left direction. This is why we call it a modal **outgoing** transmission condition.

Remark 7.1. *One can show that this condition can be rewritten using the operator* $\mathcal{T}^{-,0}_{\mathcal{Y}\to\mathcal{X}}$ *defined in* (33) *with* $l = 0$

$$\mathbf{X}^b - \mathcal{T}^{-,0}_{\mathcal{Y}\to\mathcal{X}}(\mathbf{Y}^b) = \mathbf{X}^+ - \mathcal{T}^{-,0}_{\mathcal{Y}\to\mathcal{X}}(\mathbf{Y}^+) \quad \textit{on} \quad \Gamma_a^+ \tag{47}$$

Thus, extending this definition of transmission condition on Γ_a^- the associated iterative algorithm that we finally propose is

$$\begin{cases} -\operatorname{div}\sigma(\mathbf{u}^b_{(n)}) - \omega^2\rho\,\mathbf{u}^b_{(n)} = f & \text{in } \Omega_b, \\ \sigma(\mathbf{u}^b_{(n)})\cdot\nu = 0 & \text{on } \partial\Omega\cap\partial\Omega_b, \\ \sigma(\mathbf{u}^b_{(n)})\cdot\,\nu + \alpha\,\mathbf{u}^b_{(n)} = \sigma(\mathbf{u}^\pm_{(n)})\cdot\nu + \alpha\,\mathbf{u}^\pm_{(n)} & \text{on } \Gamma_b^\pm, \end{cases}$$

$$\begin{cases} -\operatorname{div}\sigma(\mathbf{u}^\pm_{(n)}) - \omega^2\rho\,\mathbf{u}^\pm_{(n)} = 0 & \text{in } \Omega_a^\pm, \\ \sigma(\mathbf{u}^\pm_{(n)})\cdot\nu = 0 & \text{on } \partial\Omega\cap\partial\Omega_a^\pm, \\ A_k^\pm(\mathbf{u}^\pm_{(n)}) = A_k^\pm(\mathbf{u}^b_{(n-1)}),\ \forall k\geq 0 & \text{on } \Gamma_a^\pm, \end{cases} \tag{48}$$

7.2. Advantages of the method

Let us now show the main advantages of this outgoing transmission condition.

1. **Consistency of the method**. As we have seen in Section 4.2, the algorithm is consistent if the unique solution of the following problems set in B_l^- and B_l^+:

$$\begin{cases} -\operatorname{div}\sigma(\mathbf{v}^\pm) - \omega^2\rho\,\mathbf{v}^\pm = 0 & \text{in} \quad B_l^\pm, \\ \sigma(\mathbf{v}^\pm)\cdot\nu = 0 & \text{on} \quad \partial\Omega\cap\partial B_l^\pm, \\ \sigma(\mathbf{v}^\pm)\cdot\nu + \alpha\,\mathbf{v}^\pm = 0 & \text{on} \quad \Gamma_b^\pm, \\ A_k^\pm(\mathbf{v}^\pm) = 0,\ \forall k\geq 0 & \text{on} \quad \Gamma_a^\pm. \end{cases} \tag{49}$$

is the trivial solution. Let us show it for v^+. Thanks to the modal condition on Γ_a^+, we have

$$\begin{bmatrix} X(\mathbf{v}^+) \\ Y(\mathbf{v}^+) \end{bmatrix} = \sum_{k\geq 0} A_k^-(\mathbf{v}^+)\, e^{-\imath\beta_k(z-a)} \begin{bmatrix} \mathcal{X}_k(\mathbf{x}_s) \\ \mathcal{Y}_k(\mathbf{x}_s) \end{bmatrix} \quad \text{in} \quad B_l^+.$$

Then v^+ is the restriction of w^+ which is the outgoing solution in the the half-guide $\Gamma_b^+ \times \{z < b\}$ of

$$\begin{cases} -\mathrm{div}\,\sigma(\mathbf{w}^+) - \omega^2\rho\,\mathbf{w}^+ = 0 & \text{in} \quad \Gamma_b^+ \times \{z < b\}, \\ \sigma(\mathbf{w}^+)\cdot\nu = 0 & \text{on} \quad \partial\Gamma_b^+ \times \{z < b\}, \\ \sigma(\mathbf{w}^+)\cdot\nu + \alpha\,\mathbf{w}^+ = 0 & \text{on} \quad \Gamma_b^+, \end{cases}$$

Because w^+ is the outgoing solution of this homogeneous problem, it can be proved that its propagative components are equal to 0 and then w^+ is exponentially decaying. For $\alpha = 0$, non trivial solution for some particular frequencies can exist and are called edge modes [30]. For $\mathrm{Im}(\alpha) > 0$, the only solution of the above problem is the trivial solution (edge mode never exists), the proof being similar to the proof of Lemma 3.3. We refer the reader to [35] for more details.

Thus if $\mathrm{Im}(\alpha) > 0$, the algorithm is consistent. Let us emphasize in addition that the condition set on Γ_a^+ has completely eliminated the spurious effects of the boxes $B_l^\pm$: the boxes have in some sense disappeared.

2. **Convergence properties of the iterative algorithm** To explain the benefit of considering the outgoing transmission condition on the convergence of the iterative algorithm, we will again consider the case of an unperturbed half-guide (see Figure 3) for which analytical calculations can be done. We use exactly the same framework than in Section 6.1 computing the solution of (37) using the new transmission condition (46) on Γ_a. Here, we show that the corresponding λ_k's are given by

$$\lambda_k = \frac{e^{i\beta_k b}}{e^{i\beta_k b} - e^{-i\beta_k b}}. \tag{50}$$

Compared to (42), we notice a better behaviour of λ_k for large k. Indeed λ_k tends to 0 exponentially fast as $e^{-2\mathrm{Im}(\beta_k)b}$, instead of $e^{-2\mathrm{Im}(\beta_k)l}$ in the previous algorithms. Surprisingly, λ_k tends to 0 exponentially fast at least as $e^{-2\mathrm{Im}(\beta_k)a}$ independently from the size of the overlap. Consequently, we can expect a rapid convergence of the associated GMRES *quasi* independently of the size of the overlap contrary to the previous algorithms. In practice, this property enables to use a small overlap and improve the convergence of the algorithm without increasing too much the computational cost.

We have represented in Figure 5 the localization of the coefficients λ_k in the complex plane , for a waveguide of width h made of aluminium (see [31] for the coefficients of the material), at a given

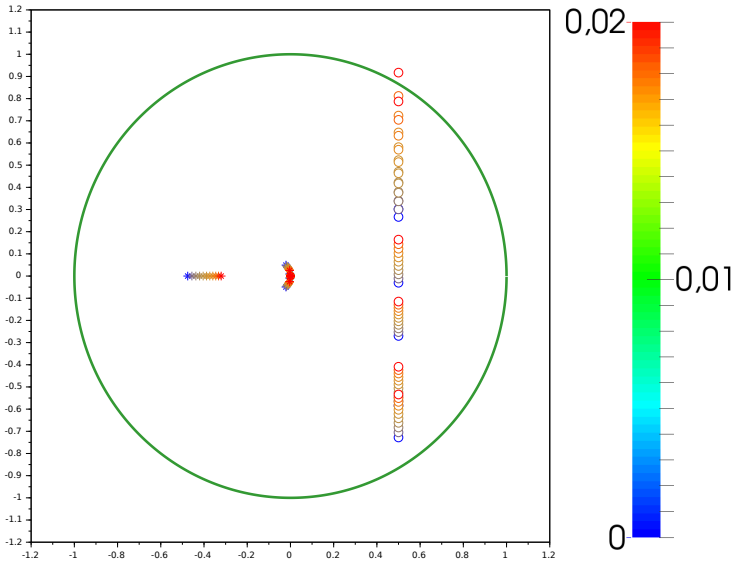

Figure 5: Localization of the coefficients λ_k in the complex plane : the color scale indicates l/h where h is the width of the waveguide and l the size of the overlap.

frequency ω and for various sizes of the overlap l. The frequency is such that there are 6 propagative modes. The coefficients related to the propagative modes (resp. evanescent modes) are represented by circles (resp. by stars). We can observe that, as explained, the λ_k's related to the evanescent modes accumulate at 0 when k tends to $+\infty$ even for the smallest overlap. Note that the coefficients related to the propagative modes have a constant real part which is equal to $1/2$.

3. **Generalization to the anisotropic case.** The modal-outgoing condition we propose to impose on the interior boundaries $\Gamma_a^{\pm}$ requires to be able to compute the amplitude $A_k^{\pm}(\mathbf{u}^b)$. In the case of general anisotropy, the Fraser's relation (4) does not hold anymore, so we cannot use the formula (45). However, using the general bi-orthogonality relations (see [1]), we can get the modal amplitudes by projection over the two families of modes (right-going and left-going):

$$A_k^{\pm}(\mathbf{u}) = \frac{1}{J_k^{\pm}} \int_{\Gamma_a^+} \mathbf{u}\,\mathcal{S}_k^{\mp} - \mathbf{t}\,\mathcal{U}_k^{\mp}, \quad \text{where} \quad J_k^{\pm} = \int_{\Gamma_a^+} \mathcal{U}_k^{\pm}\mathcal{S}_k^{\mp} - \mathcal{T}_k^{\pm}\mathcal{U}_k^{\mp}$$

where $\mathcal{S}_k^{\pm}$ represents the normal stress of the mode.

As an illustration, we have considered an artificial 2D anisotropic medium and we have computed the solution for two sizes $b/h \in \{0.5, 1\}$ of the computational area Ω_b. On Figure 6, we have repre-

sented the modulus of the displacement field obtained in these two cases. We also represent the whole solution reconstructed in the half-guides Ω_a^+ thanks to the modal expansion. As we can see on Figure

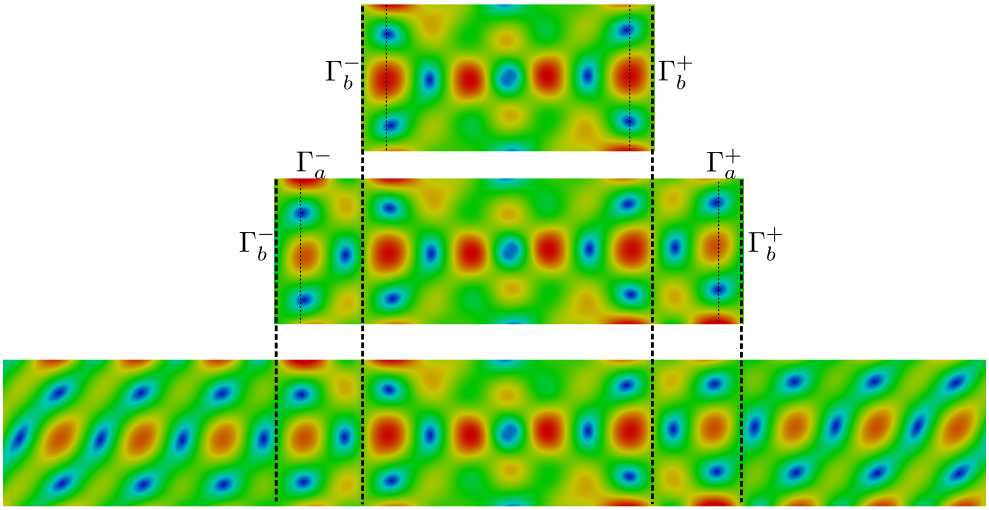

Figure 6: Modulus of the computed solution in a 2D anisotropic waveguide of width h for different Ω_b : $b = 0.5h$ (top) and $b = h$ (center) for the same overlap. Solution reconstructed in the half-guides $\Omega_a^{\pm}$ (bottom).

6, the restriction of the second computation (in the center) to the smaller domain Ω_b matches very well.

8. Implementation and numerical results

As we have seen in the previous section, the iterative algorithms that we have studied in this paper cannot be implemented directly to solve the scattering problem because the convergence is not always ensured (see Section 6). But, we propose to use GMRES algorithm (see [32]) preconditionned thanks to our iterative algorithms (we give more details on that point below). It is well known that GMRES is a Krylov subspace method (as the conjugate gradient) whose convergence is always ensured, on contrary to the classical iterative methods (namely Gauss-Seidel and Jacobi). Let us emphasize that the linear system we are led to solve is not symmetric and we cannot applied the conjugate gradient. It is widely recognized that the choice of the preconditioner is the most critical ingredient to improve the convergence of the GMRES algorithm.

8.1. Description of the method

In the discrete level, thanks to Section 5, we can show that the problem (24-26) with overlapping ($b-a>0$) can be rewritten as

$$\mathbb{A}\mathbf{U}^{\mathbf{b}}_{(\mathbf{n+1})} = \mathbb{F} - \mathbb{T}\mathbf{U}^{\mathbf{b}}_{(\mathbf{n})}. \tag{51}$$

where

- $\mathbb{F}$ is related to the source term f;
- $\mathbf{U}^b$ is expected to be an approximation of the solution in Ω^b;
- $\mathbb{A}$ is the matrix associated to the interior problem and inverting the matrix $\mathbb{A}$ corresponds to solve the problem set in Ω_b ;
- $\mathbb{T}$ is related to the operator $\mathcal{T}^{\pm,l}_{\mathcal{Y}\to\mathcal{R}}$ and the product matrix-vector $\mathbb{T}\mathbf{U}^{\mathbf{b}}_{(\mathbf{n})}$ corresponds to take the boundary data in algorithm (24-26).

As explained in Section 5, the problem (51) is an iterative algorithm to solve the direct problem

$$(\mathbb{A}+\mathbb{T})\mathbf{U}^b = \mathbb{F}. \tag{52}$$

Because the matrix T is dense, it is prohibitive for realistic problem to make the direct inversion of the matrix $\mathbb{A}+\mathbb{T}$. An iterative solving of this problem is then required.

The algorithms (51) present several advantages. First $\mathbb{A}$ is a sparse matrix, its inversion is relatively cheap. Secondly, the product matrix-vector is a simple modal decomposition, which can be achieved efficiently without assembling the matrix $\mathbb{T}$ (the number of operations is of order $N_S \times M$ where N_S is the number of dof in S and M is the number of significant modes instead of N_S^2 with assembling).

But again this iterative algorithm does not always converge, as we have seen in Section 6. The idea then is to use GMRES with $\mathbb{A}^{-1}$ as the preconditioner. It is a good preconditioner because it is cheap to construct and the preconditioned iteration converges rapidly as we will see in the next section.

8.2. Convergence of the preconditioned GMRES

The convergence properties of the GMRES preconditioned by $\mathbb{A}^{-1}$ are linked to the position of the eigenvalues of the matrix $\mathbb{M} = (\mathbb{I} + \mathbb{A}^{-1}\mathbb{T})$, as explained in [32] for instance. More precisely, let us remind that if $\mathbb{M}$ a diagonalizable matrix then the residual norm provided at the mth step of GMRES satisfies

$$\| r_{(m+1)} \| \leq \kappa(\mathbb{M}) \| r_{(0)} \| \min_{p\in P_m} \left(\max_{\lambda\in\sigma(\mathbb{M})} |p(\lambda)| \right) \tag{53}$$

where $\kappa(\mathbb{M})$ depends on the spectral decomposition of $\mathbb{M}$, $\sigma(\mathbb{M})$ is the set of its eigenvalues and P_m is the set of polynomial p of degree at most m such that $p(0) = 1$. In other words, the convergence of the GMRES depends on the number of cluster points of the set $\sigma(\mathbb{M})$.

Here, as explained in Section 6.2, the operator $\mathcal{T}^{\pm,l}_{\mathcal{Y}\to\mathcal{R}}$ is compact in presence of overlap (see Proposition 6.1). In consequence, their eigenvalues tend to zero (the decay is in fact exponential). Thus, the eigenvalues of

the associated matrix $\mathbb{T}$ (which are an approximation of the eigenvalues of the operators $\mathcal{T}^{\pm,l}_{\mathcal{V}\to\mathcal{R}}$) concentrate around zero. Therefore, the eigenvalues of $\mathbb{M}$ are clustered around 1 and, for that reason, our choice of preconditioners is relevant.

The same properties hold for the transmission condition (25) and outgoing transmission condition defined in Section 7.

8.3. 2D numerical results

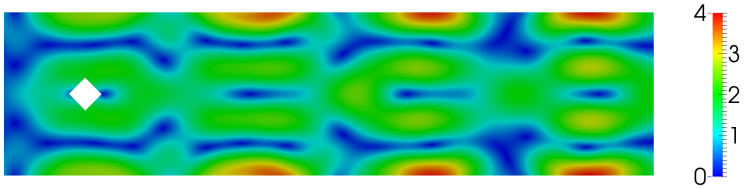

Figure 7: Modulus of the reconstructed solution in a semi-infinite waveguide made of aluminium of width h.

We consider a 2D semi-infinite waveguide of width h, made of aluminium (see [31] for the coefficients of the material) containing a square cavity. Figure 7 represents the computed solution at a frequency such that there are 4 propagative modes and we consider 20 evanescent modes in our computation.

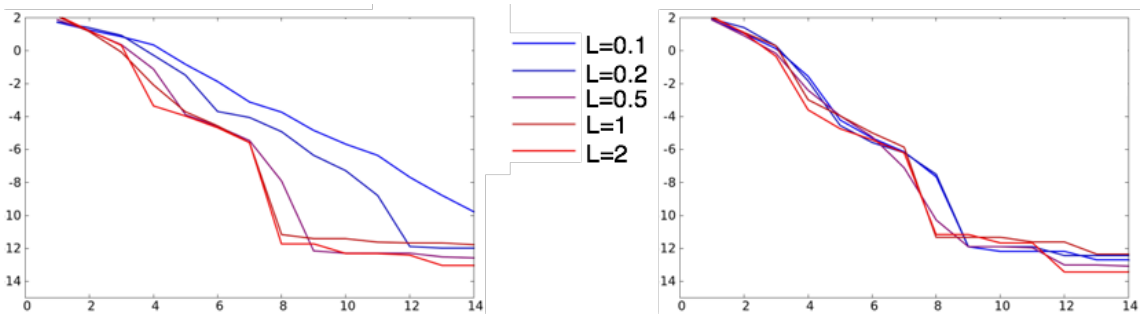

Figure 8: Evolution of the residual error versus the iteration of GMRES for various values of l/h where h is the width of the waveguide and l the size of the overlap : using the transmission condition (26) (left figure) and (46) (right figure).

For this configuration, we compare the efficiency of the GMRES algorithm for two choices of transmission conditions and different sizes of the overlap. Figure 8 represents the evolution of the residual error $\| MU^b - b \|$ versus the iteration of GMRES for various sizes of overlap l. As we can see, increasing l makes the algorithm have a sharper convergence (up to the machine precision) if we use the transmission conditions (26) (see left figure). But if we use the 'outgoing' transmission condition (46) (see right figure), the effect of

a small overlap on the convergence is more important than considering (26). As expected, the efficiency is obtained directly with the smallest overlap.

8.4. Numerical Results for 3D geometries

We consider now one more realistic problem : a tube of diameter 115 mm and thickness 7.5 mm is locally perturbed because of corrosion, see Figure 9.

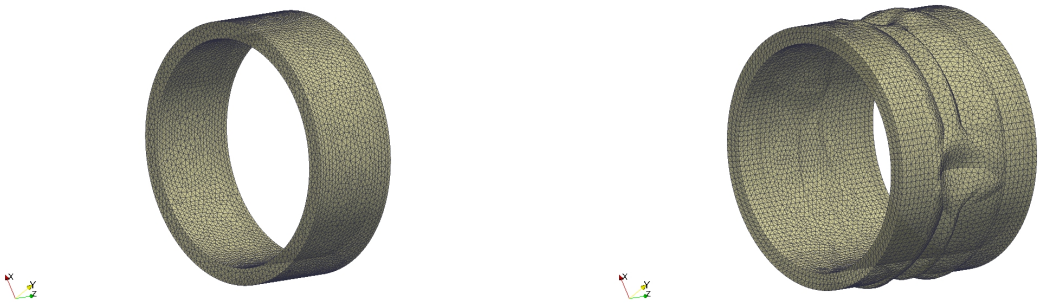

Figure 9: Mesh of the regular part (left figure) and the rusted part (right figure) of the tube.

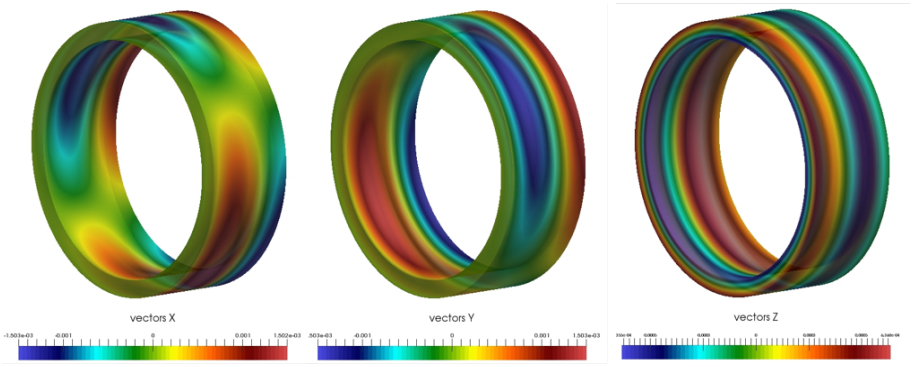

Figure 10: The three components of the incident field (u_x, u_y, u_z).

The frequency $\omega = 0.025Mhz$ is such that there exist 21 propagative modes and we consider 79 evanescent modes in our computations. Let us point out that a pre-processing step based on a SAFE method [19] enables to compute numerically the modes of the problem. We consider the diffraction problem for an incident field which is the first compressional mode, represented in Figure 10. Figures 11 represent the 3 components of the displacement around the perturbation.

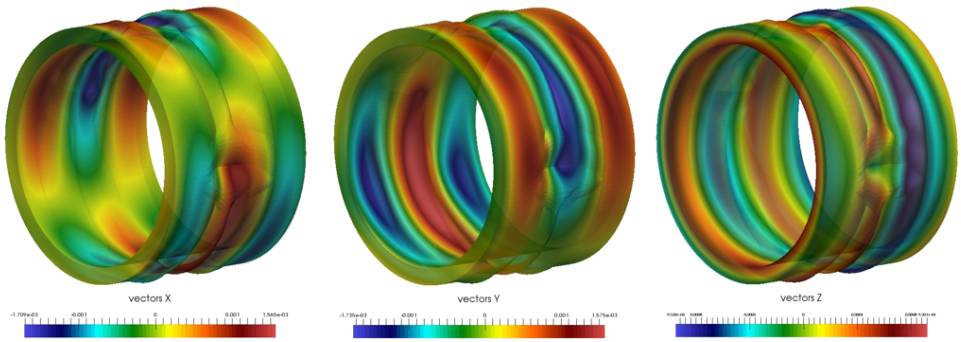

Figure 11: The three components of the displacement around the perturbation for the problem (i).

In Figure 12, we compare, as in the 2D case, the efficiency of the GMRES algorithm for the same two different transmission conditions and different sizes of the overlap. The conclusions are the same than in the 2D case.

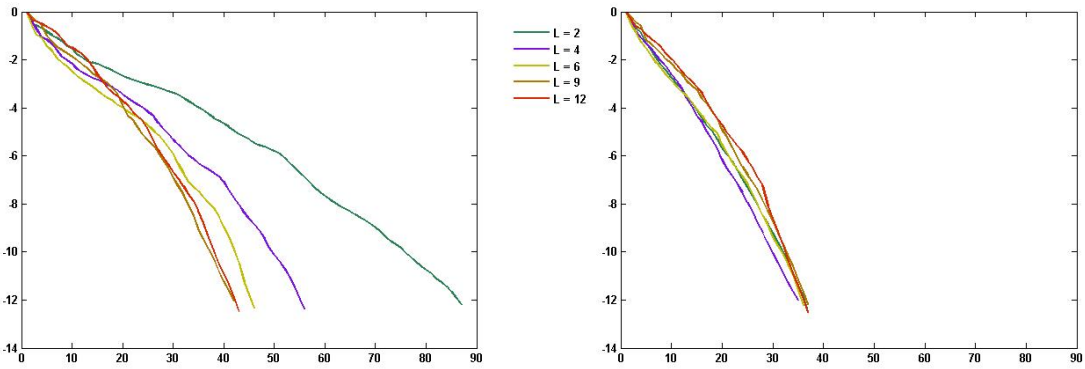

Figure 12: Evolution of the residual error versus the iteration of GMRES for various values of l/h where h is the width of the waveguide and l the size of the overlap, using the transmission condition (26) (left figure) and (46) (right figure)

We compare the computational time of the method using the transmission conditions (26) or (46) for different values of the overlap using the associated preconditionned GMRES algorithm (see Figure 13). We represent in red the computational time for the factorization of the preconditionner (which is the same for the two transmission conditions). It increases with the overlap which is due to the fact that the interior domain Ω^b (and then the size of the matrix) increases. Then we compare the remaining computational time for two transmission conditions, which corresponds to the product matrix-vector, multiplied by the number of iterations. For a given overlap, the number of iterations of the GMRES algorithm is smaller for the second choice of transmission condition : it seems to be the best option! Moreover, for the first choice of

transmission condition, the computational time first decreases with the overlap : this is one of the advantage of considering overlaps. However for large overlaps, it increases with the overlap. The size of the matrix being bigger and bigger, the product matrix-vector spends more time at each iteration of the algorithm. For the second choice of transmission condition, the advantage of the overlap is obtained for the smallest overlap. Considering bigger and bigger overlaps then deteriorates the computational time.

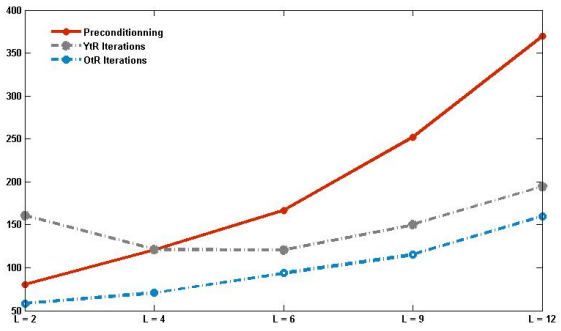

Figure 13: Comparison of the computational time.

Appendix A. Proof of Proposition 4.4

We prove here that if ω is an eigenfrequency of (30-25), then the limit problem (28-25) admits solutions that do not satisfy the compatibility relations (29).

Let us consider k_0 such that

$$v^+ = e^{\imath\beta_{k_0}(z-a)}\mathcal{U}^+_{k_0} - e^{-\imath\beta_{k_0}(z-a)}\mathcal{U}^-_{k_0},$$

is a non-zero solution of the equations (30-25) in B_l^+ (see Lemma 4.3).

We want to find $(\mathbf{u}^-, \mathbf{u}^b, \mathbf{u}^+)$ solution of (28-25) such that $\mathbf{u}^b - \mathbf{u}^- = 0$ in B_l^- and $\mathbf{u}^b - \mathbf{u}^+ = \mathbf{v}^+$ in B_l^+. The idea is to consider the diffraction problem in Ω taking

$$\mathbf{u}_{inc} = e^{-\imath\beta_{k_0}(z-a)}\mathcal{U}^-_{k_0}$$

as incident field. Then the total field $\mathbf{u}$ is such that $\mathbf{u} = \mathbf{u}_{\text{inc}} + \mathbf{u}_{\text{dif}}$ where the diffracted field $\mathbf{u}_{\text{dif}}$ is outgoing. Finally, setting

$$\mathbf{u}^- = \mathbf{u}\Big|_{\Omega_a^-}, \quad \mathbf{u}^b = \mathbf{u}\Big|_{\Omega_b}, \quad \text{and} \quad \mathbf{u}^+ = \mathbf{u}_{\text{dif}} + e^{\imath\beta_{k_0}(z-a)}\mathcal{U}^+_{k_0}$$

we get a solution of (28-25) which does not satisfy compatibility relations (29).

Appendix B. Variational formulations...

Appendix B.1. ... in absence of overlaps

We consider the following problem set in the bounded domain Ω_a:

$$\left\{\begin{array}{ll} -\mathrm{div}\,\sigma(\mathbf{u}^a) - \omega^2\rho\mathbf{u}^a = \tilde{\mathbf{f}} & \text{in } \Omega_a, \\ \sigma(\mathbf{u}^a).\nu = 0 & \text{on } \partial\Omega \cap \partial\Omega_a, \\ \mathbf{X}^a = \widetilde{\mathbf{X}} & \text{on } \Gamma_a^{\pm} \end{array}\right. \tag{B.1}$$

where $\mathbf{u}^a$ is the unknown and $\tilde{\mathbf{f}}$, $\tilde{\mathbf{g}}$ and $\widetilde{\mathbf{X}}$ are given. Let us recall that the condition $\mathbf{X}^a = \widetilde{\mathbf{X}}$ is a hybrid condition which can be rewritten as

$$\mathbf{t}_S^a = \tilde{\mathbf{t}}_S \quad \text{and} \quad u_z^a = \tilde{u}_z$$

Classically, the Dirichlet condition $u_z^a = \tilde{u}_z$ is taken into account by introducing any lifting function $\mathbf{w}^a$ such that

$$w_z^a = \tilde{u}_z \quad \text{on } \Gamma_a^{\pm}$$

and writing a new problem for the unknown $\mathbf{u}^a - \mathbf{w}^a$ with a homogeneous Dirichlet boundary condition on $\Gamma_a^{\pm}$. Then we are led to consider the case where

$$\tilde{u}_z = 0 \tag{B.2}$$

and we have the

Lemma Appendix B.1. *If (B.2) holds, problem (B.1) has the following equivalent variational form:*

$$\left|\begin{array}{l} \mathbf{u}^a \in V_a \text{ such that } \forall \mathbf{v} \in V_a \\ a(\mathbf{u}^a, \mathbf{v}) - \omega^2 m(\mathbf{u}^a, \mathbf{v}) = \displaystyle\int_{\Omega_a} \tilde{\mathbf{f}} \cdot \mathbf{v} + \int_{\Gamma_a^+} \tilde{\mathbf{t}}_S \cdot \mathbf{v}_S - \int_{\Gamma_a^-} \tilde{\mathbf{t}}_S \cdot \mathbf{v}_S \end{array}\right. \tag{B.3}$$

where $V_a = \{\mathbf{v} \in \mathbf{H}^1(\Omega_a);\ v_z = 0 \text{ on } \Gamma_a^{\pm}\}$,

$$a(\mathbf{u}, \mathbf{v}) = \int_{\Omega_a} \sigma(\mathbf{u}) : \varepsilon(\mathbf{v}) \quad \text{and} \quad m(\mathbf{u}, \mathbf{v}) = \int_{\Omega_a} \rho\mathbf{u} \cdot \mathbf{v}.$$

Moreover, problem (B.3) is well-posed except for a countable set of frequencies tending to infinity.

Proof: Multiplying the first equation of (B.1) by $\mathbf{v} \in V$, integrating on Ω_a and applying a Green formula, we get:

$$\begin{array}{rl} a(\mathbf{u}^a, \mathbf{v}) - \omega^2 m(\mathbf{u}^a, \mathbf{v}) = & \displaystyle\int_{\Omega_a} \tilde{\mathbf{f}} \cdot \mathbf{v} + \int_{\Gamma_a^+} (\sigma(\mathbf{u}^a)\nu)_S \cdot \mathbf{v}_S + \int_{\Gamma_a^+} (\sigma(\mathbf{u}^a)\nu)_z \cdot v_z \\ & - \displaystyle\int_{\Gamma_a^-} (\sigma(\mathbf{u}^a)\nu)_S \mathbf{v}_S - \int_{\Gamma_a^-} (\sigma(\mathbf{u}^a)\nu)_z \cdot v_z. \end{array}$$

But for $\mathbf{v} \in V$, $v_z = 0$ on $\Gamma_a^{\pm}$, so that two integrals disappear. The two other ones can be modified by using the data. Finally, the bilinear form $a(\mathbf{u}, \mathbf{v})$ is coercive on V_a, by virtue of Korn's inequality. The lemma

follows by a classical result of spectral theory. ■

Appendix B.2. ... in presence of overlaps

To derive a standard variational formulation for the problem (35), we must give a weak sense to the term $\mathbf{Y}^b = \left[\mathbf{u}_s^b,\ t_z^b\right]$. The difficulty comes from the normal derivative t_z^b on $\Gamma_a^{\pm}$ which appears in integrals of type

$$\int_{\Gamma_a^{\pm}} t_z^b(\mathcal{U}_k)_z$$

which has no sense in the discrete point of view. To do so, we introduce a lifting function $\mathcal{L}(\mathcal{U}_k)$ in B_l^+ that verifies:

1. $(\mathcal{L}(\mathcal{U}_k))_z = (\mathcal{U}_k)_z$ and $(\mathcal{L}(\mathcal{U}_k))_S = 0$ on the boundary Γ_a^+,
2. $\mathcal{L}(\mathcal{U}_k) = 0$ on Γ_b^+,
3. and $\mathcal{L}(\mathcal{U}_k)$ is smooth enough.

Thus, by the Green's formula, it comes that:

$$\int_{\Gamma_a^{\pm}} t_z^b(\mathcal{U}_k)_z = \int_{\Gamma_a^{\pm}} t^b\mathcal{L}(\mathcal{U}_k) = \int_{B_l^+} -\mathrm{div}\,\sigma(\mathbf{u}^b)\cdot\mathcal{L}(\mathcal{U}_k) - \sigma(\mathbf{u}^b) : \varepsilon(\mathcal{L}(\mathcal{U}_k)). \tag{B.4}$$

Finally, using the fact that $\mathrm{div}\,\sigma(\mathbf{u}^b) = -\omega^2\mathbf{u}^b$ in B_l^+, we can rewrite (B.4) as follows:

$$\int_{\Gamma_a^{\pm}} t_z^b(\mathcal{U}_k)_z = \int_{\Gamma_a^{\pm}} t^b\mathcal{L}(\mathcal{U}_k) = \omega^2\int_{B_l^+} \mathbf{u}^b\cdot\mathcal{L}(\mathcal{U}_k) - \sigma(\mathbf{u}^b) : \varepsilon(\mathcal{L}(\mathcal{U}_k)). \tag{B.5}$$

[1] Auld B.A., *Acoustic fields and waves in solids*, Krieger publishing company, Florida, 1973.

[2] Baronian V., *Couplage des méthodes modale et éléments finis pour la diffraction des ondes élastiques guidées. Application au Contrôle Non Destructif*. PhD thesis, Ecole Polytechnique, 2009.

[3] Baronian V., Jezzine K. and Le Bourdais F., *Hybrid modal/FE simulation of guided waves inspections*. AIP Conf. Proc. 1511, 191, http://dx.doi.org/10.1063/1.4789048, 2013.

[4] Baronian V., Bonnet-Ben Dhia A.-S. and Lunéville E., *Transparent boundary conditions for the harmonic diffraction problem in an elastic waveguide*. J. Comput. Appl. Math., 234(6), 1945-1952, 2010.

[5] Baronian V., Lhémery A. and Bonnet-Ben Dhia A.-S. , *Simulation of non-destructive inspections and acoustic emission measurements involving guided waves*. J. Phys.: Conf. Ser., 195, 2009.

[6] Bonnet-Ben Dhia A.-S., Chambeyron C. and Legendre G., *On the use of perfectly matched layers in the presence of long or backward guided elastic waves*, Wave Motion, vol. 51(2), 266-283, 2014.

[7] Boudendir Y., *Techniques de dcomposition de domaine et mthode d'quations intgrales*, PhD thesis, INSA Toulouse, 2002.

[8] Drozdz M., Moreau L., Castaings M., Lowe M.J.S. and Cawley P. , *Efficient Numerical Modelling of Absorbing Regions for Boundaries Of Guided Waves Problems*. AIP Conf. Proc. 820, 126, 2006.

[9] Collino F., Ghameni S., Joly P., *Domain decomposition method for harmonic wave propagation: a general presentation*. J. Comput. meth. Appl. Mech. and Eng 184(2-4), 171-211, 2000.

[10] Després B., *Méthodes de décomposition de domaine pour les problèmes de propagation d'ondes en régime harmonique*. PhD thesis, Université Paris IX Dauphine, 1991.

[11] Fraser W.B., *Orthogonality relation for the Rayleigh-Lamb modes of vibration of a plate*. J. Acoust. Soc. Am. 59, 215-216, 1976.

[12] Gander M. J. and Zhang H., *Optimized Schwarz methods with overlap for the Helmholtz equation*, Domain Decomposition Methods in Sci. and Eng. XXI, 207-215, Springer International Publishing 2014.

[13] Givoli D. *Numerical Methods for Problems in Infinite Domains*. Elsevier Science Publishers, 1992.

[14] Ben Belgacem F., Fournié M., Gmati N. and Jelassi F., *On the Schwarz algorithms for elliptic exterior boundary value problems*, ESAIM-M2AN 39(4), 693-714, 2005.doi:10.1051/m2an:2005030

[15] Gmati N. and Zrelli N. *Numerical study of some iterative solvers for acoustics in unbounded domains*, ARIMA 4, 1-23, 2006.

[16] Ben Belgacem F., Jelassi F. and Gmati N., *Convergence bounds of GMRES with Schwarz preconditionner for the scattering problem*. Int. J. Numer. Meth. Eng. 80(2), 191-209, 2009.

[17] Gravenkamp H., Prager J., Saputra AA., Song C., *The simulation of Lamb waves in a cracked plate using the scaled boundary finite element method*. J Acoust Soc Am. 132(3), 1358-1367, 2012. doi: 10.1121/1.4740478.

[18] Gregory R.D. , *A note on bi-orthogonality relations for elastic cylinders of general cross section*. J. Elasticity 13(3), 351-355, 1983.

[19] Hayashi T. and Rose J. L., *Guided wave simulation and visualisation by a semi-analytical finite element method*, Mat. Eval. 61, 7579, 2003.

[20] Kostyuchenko A.G. and Orazov M.B., *Problem of oscillations of an elastic half cylinder and related self-adjoint quadratic pencils*, Journal of Soviet Mathematics 33(3), 1025-1065, 1986. doi:10.1007/BF01085045

[21] Lions P.L., *On the Schwarz alternating method. I*, First international symposium on domain decomposition methods for partial differential equations, p 1-42, 1988.

[22] Lowe M.J.S., Alleyne D.N. and Cawley P. , *Defect detection in pipes using guided waves*. ULTRASONICS 36, 147-154, 1998.

[23] Lowe M.J.S. and Cawley P. *Long Range Guided Wave Inspection Usage Current Commercial Capabilities and Research Directions*, Int. Report, Imperial College London, 2006.

[24] Mencik J.-M. and Ichchou M. N. *Multi-mode propagation and diffusion in structures through finite elements* European Journal of Mechanics - A/Solids 24(5), 877-898, 2005.

[25] Merkulov L. G., Rokhlin S. I. and Zobnin O. P. , *Calculation of the spectrum of wave numbers for Lamb waves in a plate*, Soviet J. Nondestructive Testing 6, 369373, 1970.

[26] Halla, M. and Nannen, L.,*Hardy space infinite elements for time-harmonic two-dimensional elastic waveguide problems*, submitted, 2014.

[27] Pagneux V. and Maurel A. , *Lamb wave propagation in inhomogeneous elastic waveguides. Proceedings of the Royal Society of London. Series A: Mathematical, Physical and Engineering Sciences* 458(2024), 1913-1930, 2002.

[28] Pagneux V. and Maurel A. , *Scattering matrix properties with evanescent modes for waveguides in fluids and solids*. J. Acoust. Soc. Am. 116, 1913-1920, 2004.

[29] Pagneux V. and Maurel A. , *Lamb wave propagation in elastic waveguides with variable thickness*. Proceedings of the Royal Society A: Mathematical, Physical and Engineering Science 462(2068), 1315-1339, 2006.

[30] Pagneux, V. , *Revisiting the edge resonance for Lamb waves in a semi-infinite plate*. The Journal of the Acoustical Society of America 120(2), 649-656, 2006.

[31] Royer D., Dieulesaint E., *Ondes lastiques dans les solides*, Tome 1, Masson, 1996.

[32] Saad Y. and Schultz M.H., *GMRES: A generalized minimal residual algorithm for solving non-symmetric linear systems.*

SIAM Journal on scientific and statistical computing 7(3), 856-869, 1986.

[33] Schwarz H.A., *Ueber einige Abbildungsaufgaben.* J. fr die reine und angewandte Mathematik, 1869.

[34] Skelton E. A. , Adams S. D.M., and Craster R. V. , *Guided elastic waves and perfectly matched layers.* Wave Motion, 44(7-8), 573-592, 2007.

[35] Tonnoir A., *Conditions transparentes pour la diffraction d'ondes en milieu lastique anisotrope.* PhD Thesis, Ecole Polytechnique, 2015.

[36] Benmeddour F., Treyssède F. and Laguerre L., *Numerical modeling of guided wave interaction with non- axisymmetric cracks in elastic cylinders*, Int. J. Solids Structures 48 (5), 764774, 2011. doi:10.1016/j. ijsolstr.2010.11.013.

[37] Treyssède F., *Mode propagation in curved waveguides and scattering by inhomogeneities: application to the elastodynamics of helical structures.* J Acoust Soc Am. 129(4), 1857-68, 2011. doi: 10.1121/1.3559682.

[38] Nakamura G., Uhlmann G. and Wang J.-N., *Unique Continuation for Elliptic Systems and Crack Determination in Anisotropic Elasticity* Contemp. Math. 362, 321-338, 2004.